

Supplementary Material

Gravimetric detection of sinkhole hazard at abandoned coal mine Čárý (Slovakia) using Growth inversion – preliminary results

Jozef Bódi, Peter Vajda, Pavol Zahorec, Roman Pašteka, Juraj Papčo, René Putiška, Bibiana Brixová, José Fernández

Growth models Čárý

Homogenous Growth models with $\Delta\rho = -2200 \text{ kg/m}^3$, aimed at cavities

We used the residual CBA data of Zahorec et al. (2021), as shown in figure 2 of the main paper, in our Growth inversions. First, we sought homogenous solutions with a **density contrast of 2200 kg/m^3** , aimed at **seeking cavities**, applying GROWTH-dg. We used an average cell size of 8 m (suggested default value was 8.3 m). Growth suggested the default value for the balance factor $\lambda = 30$. We tried also lower and higher values.

In figure B1 we present a homogenous solution with $\Delta\rho = -2200 \text{ kg/m}^3$, $\lambda = 15$, no trend co-adjustment, no reweighting of residuals ($B = 8$), and no depth weighting ($D = 0$). This solution is overfitting (misfit: rms = $7 \text{ } \mu\text{Gal}$, max = $24 \text{ } \mu\text{Gal}$).

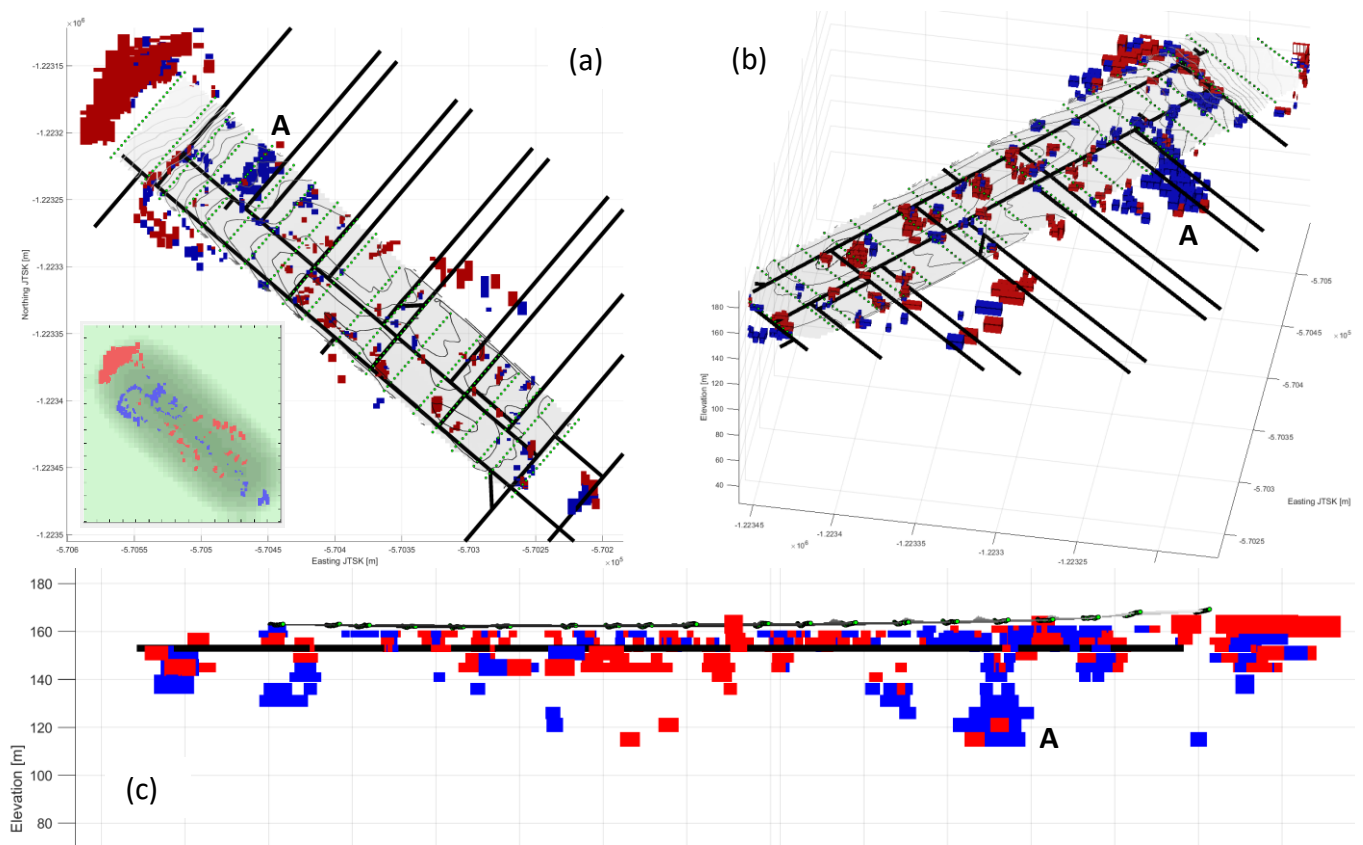
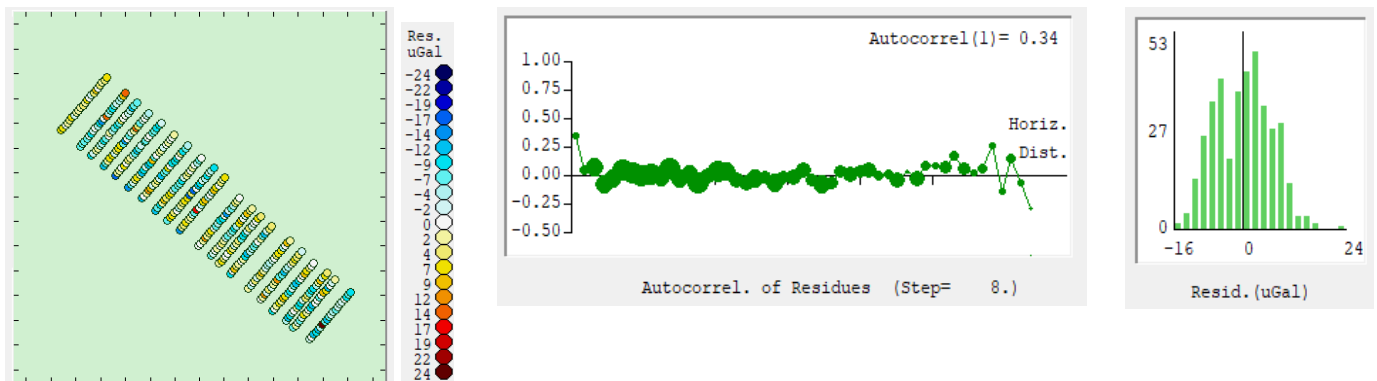


Figure B1

Overfitting ($\lambda=15$) homogenous model ($\Delta\rho = -2200 \text{ kg/m}^3$) with no trend co-adjustment, no residual reweighting ($B = 8$), and no depth weighting ($D = 0$). (a) top view (az. = 0, el. = 90), (b) 3D view from roughly NE (az. = 100, el. = 40), (c) lateral view from NE (az. = 135, el. = 0). Bold black lines represent access corridors. Inset in (a) is top view from Growth running screen.



This solution is strongly overfitting (misfit: rms = $7 \text{ } \mu\text{Gal}$, max = $24 \text{ } \mu\text{Gal}$)

Although this solution may be polluted by artifacts due to strong overfitting, it seems to indicate small linearly aligned cavities between the surface and the level of the corridors, aligned along access corridor 2, and partly (in the NW part) also along corridor 1, and along the corridor joining these two in the NW part. This solution indicates also a deeper source body (labelled “A”) at the depth of about 40 m below surface, related to the pronounced gravity low (labelled “A” in figure 2 of the main paper). This source cannot represent void space, as it could not be reasoned out at this place and such depth. It will be explored further.

In figure B2 we present a homogenous solution with $\Delta\rho = -2200 \text{ kg/m}^3$, $\lambda = 30$, no trend co-adjustment, no reweighting of residuals ($B = 8$), and no depth weighting ($D = 0$). This solution is a good-fit compact solution (misfit: rms = 15 μGal , max = 42 μGal).

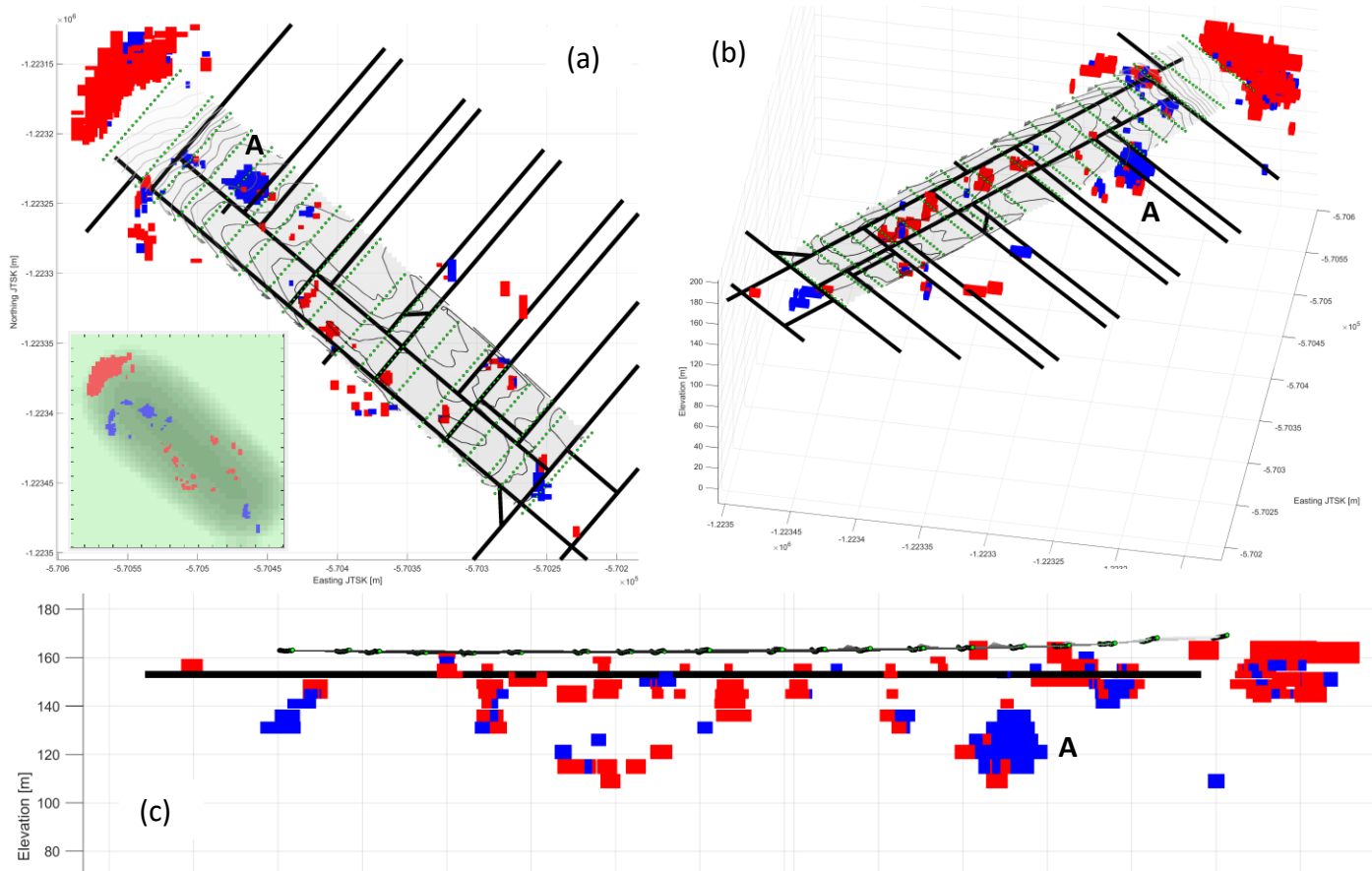
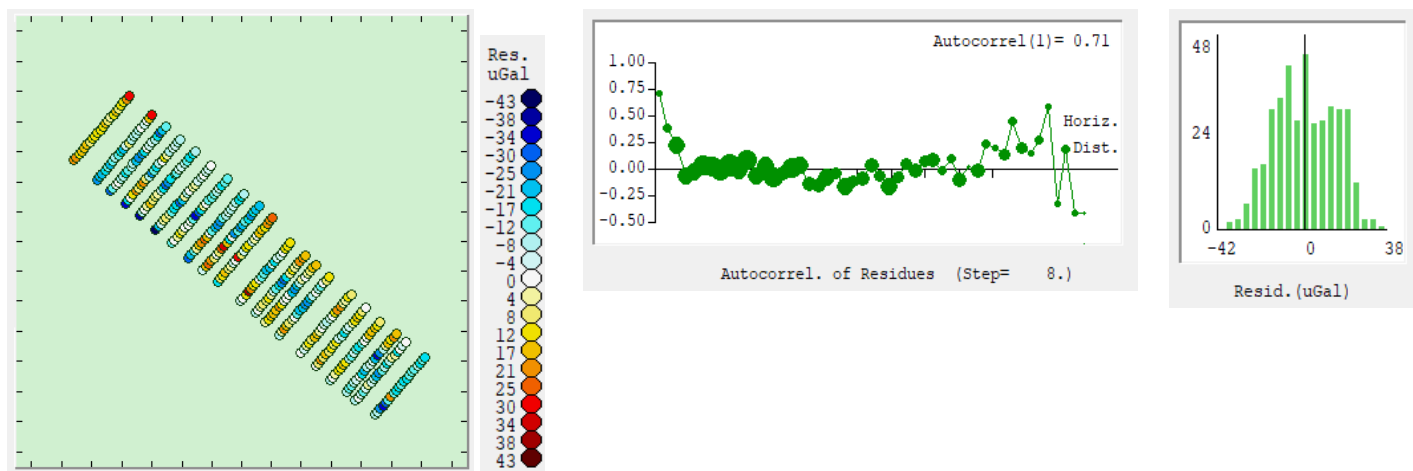


Figure B2

Good-fit compact ($\lambda = 30$) homogenous model ($\Delta\rho = -2200 \text{ kg/m}^3$) with no trend co-adjustment, no residual reweighting ($B = 8$), and no depth weighting ($D = 0$). (a) top view (az. = 0, el. = 90), (b) 3D view from roughly NE (az. = 100, el. = 40), (c) lateral view from NE (az. = 135, el. = 0). Bold black lines represent access corridors. Inset in (a) is top view from Growth running screen.



This solution has adequate fit (misfit: rms = 15 μGal , max = 42 μGal)

This solution is compact with adequate fit. It still seems to indicate some small cavities between the surface and the level of the corridors in the NW part of the data area. This solution indicates even clearly a deeper source body (labelled “A”) at the depth of about 40 m below surface. Now the body is more compact compared to figure B1.

We also ran the inversions presented in [figures B1](#) and [B2](#) with the functionality for trend co-adjustment switched on. The co-adjusted trend was insignificant. It had no impact on the solutions presented in [figures B1](#) and [B2](#).

Homogenous Growth models with $\Delta\rho = -300 \text{ kg/m}^3$, aimed at geological structural sources

Next, we sought homogenous solutions with a **density contrast of 300 kg/m^3** , aimed at **seeking structural geological sources, partly collapsed/filled cavities, or surface collapses filled with tailings**, applying GROWTH-dg. We used an average cell size of 8 m (suggested default value was 8.3 m). Growth suggested the default value for the balance factor $\lambda=50$. We tried also lower and higher values.

In [figure B3](#) we present a homogenous solution with $\Delta\rho = -300 \text{ kg/m}^3$, $\lambda = 15$, no trend co-adjustment, no reweighting of residuals ($B = 8$), and no depth weighting ($D = 0$). This solution is a strongly overfitting solution (misfit: rms = $3 \text{ }\mu\text{Gal}$, max = $15 \text{ }\mu\text{Gal}$).

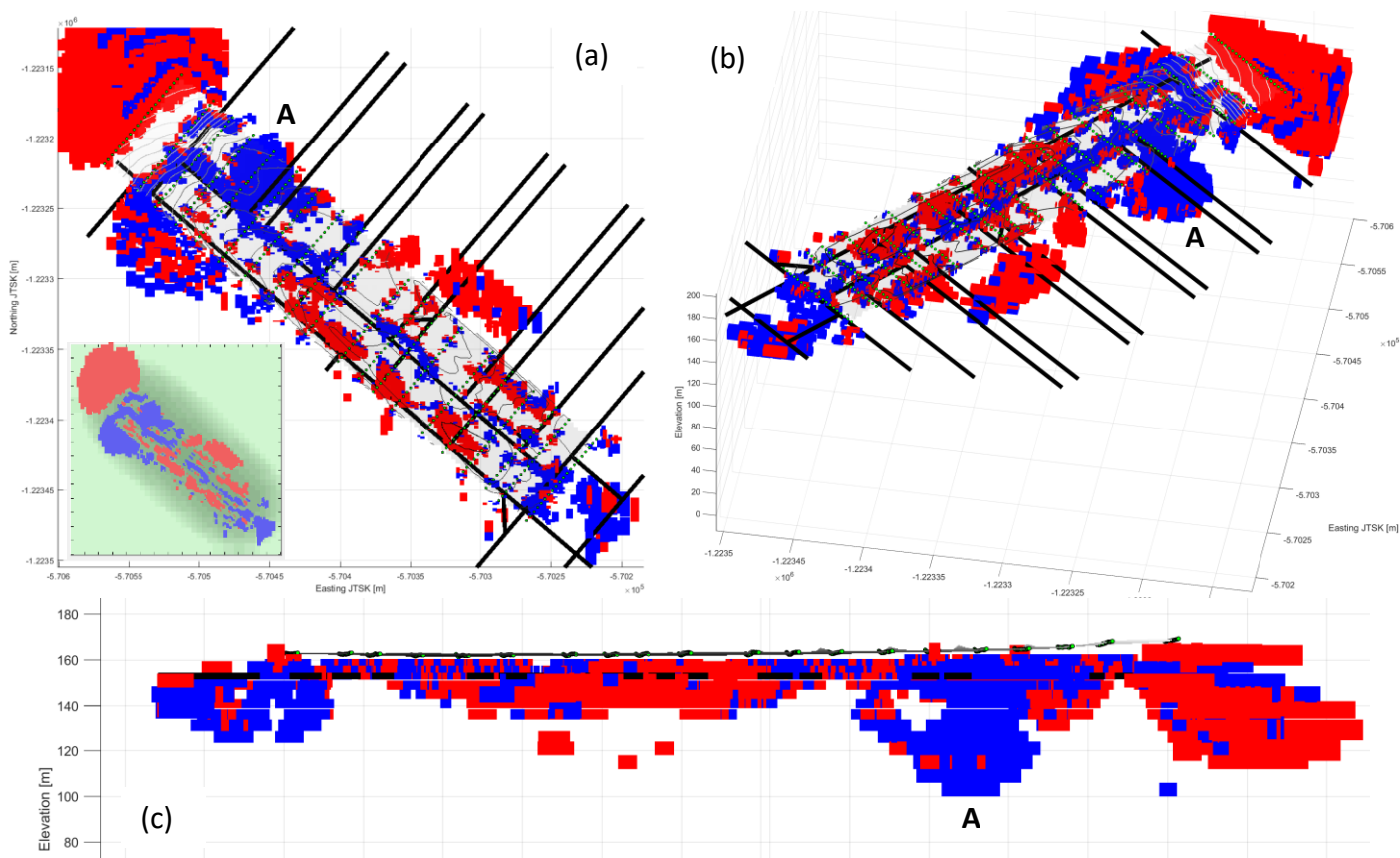
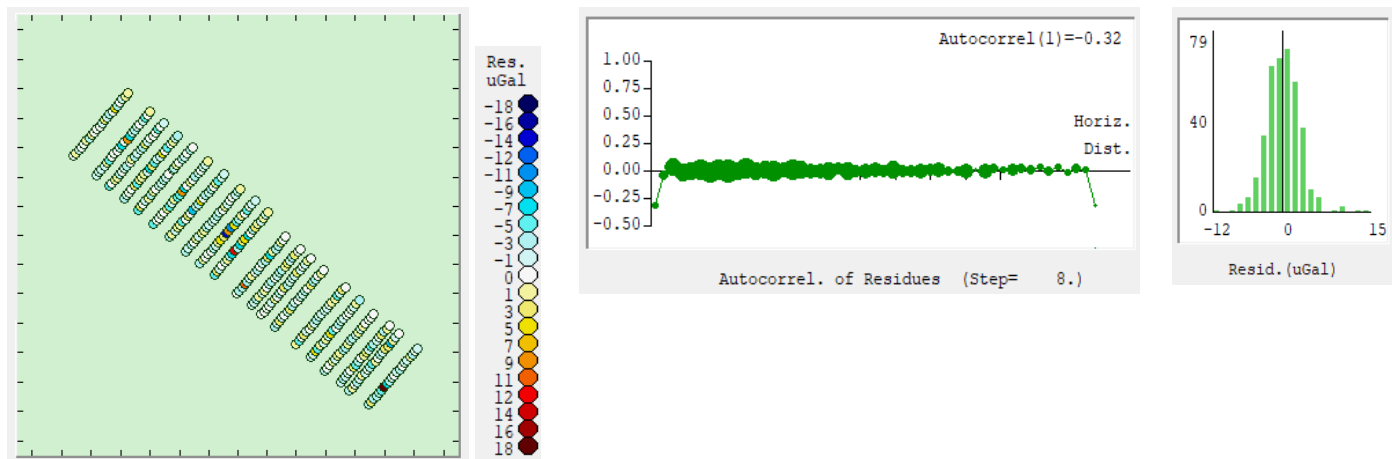


Figure B3

Strongly over-fitting ($\lambda=15$) homogenous model ($\Delta\rho = -300 \text{ kg/m}^3$) with no trend co-adjustment, no residual reweighting ($B = 8$), and no depth weighting ($D = 0$). (a) top view (az. = 0, el. = 90), (b) 3D view from roughly NE (az. = 100, el. = 40), (c) lateral view from NE (az. = 135, el. = 0). Bold black lines represent access corridors. Inset in (a) is top view from Growth running screen.



This solution has strong over-fit (misfit: rms = $3 \text{ }\mu\text{Gal}$, max = $15 \text{ }\mu\text{Gal}$)

This solution is strongly overfitting. The source bodies are relatively inflated compared to the previous solutions. Due to the smaller density contrast, the shallow linearly aligned cavities between the surface and the level of the

corridors, associated with access corridor 2, are very clearly pronounced and appear nearly continuous along the entire corridor. Same holds true for the short corridor connecting corridors 1 and 2 in the NW part. Sporadic shallow cavities appear also along corridor 1. The deep source ("A") is present and more inflated in this solution. Due to the selected density contrast the cavities should be interpreted as partly or nearly fully filled due to collapses.

In [figure B4](#) we present a homogenous solution with $\Delta\rho = -300 \text{ kg/m}^3$, $\lambda = 50$, no trend co-adjustment, no reweighting of residuals ($B = 8$), and no depth weighting ($D = 0$). This solution is a tight-fit solution (misfit: rms = 10 μGal , max = 28 μGal).

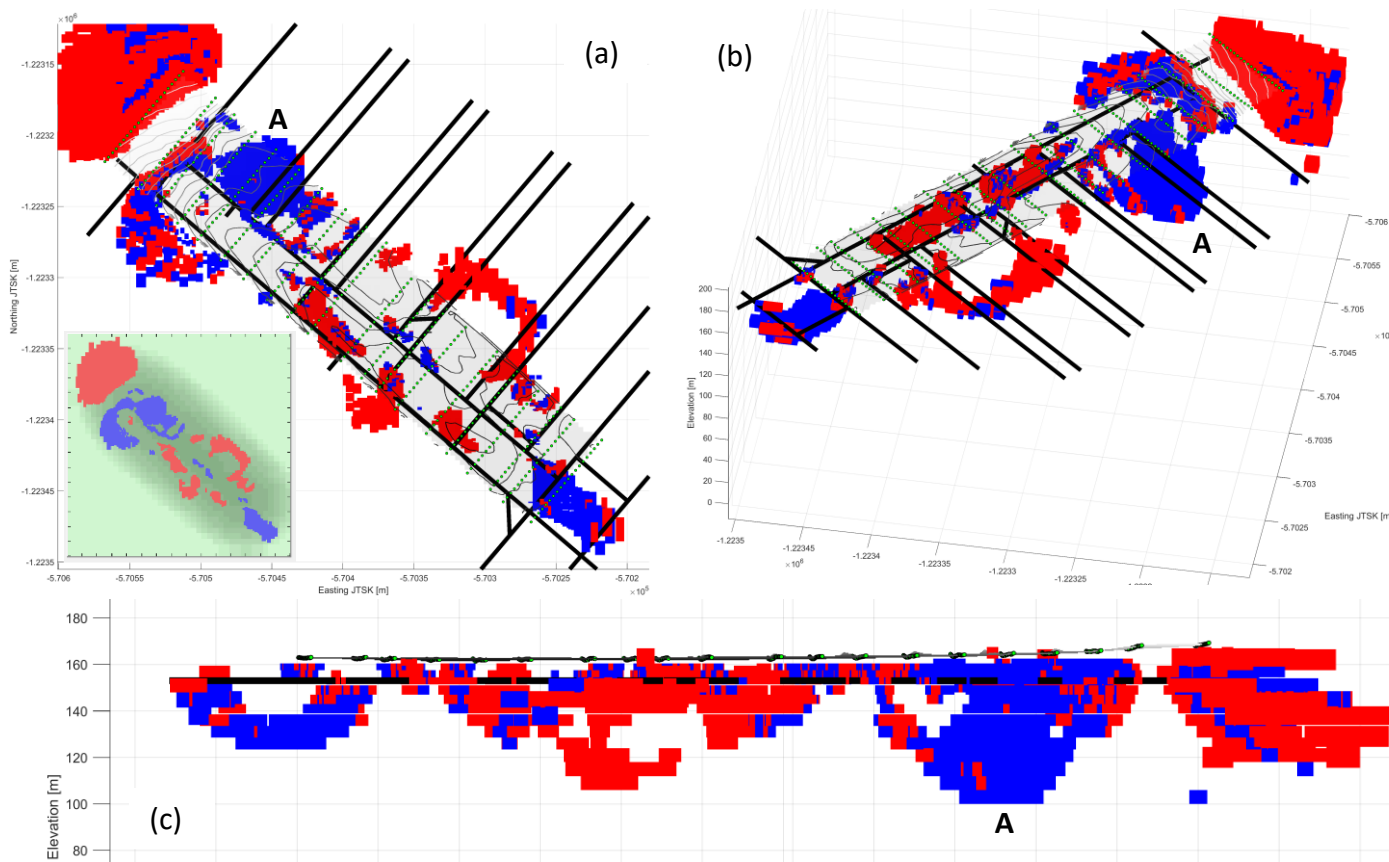
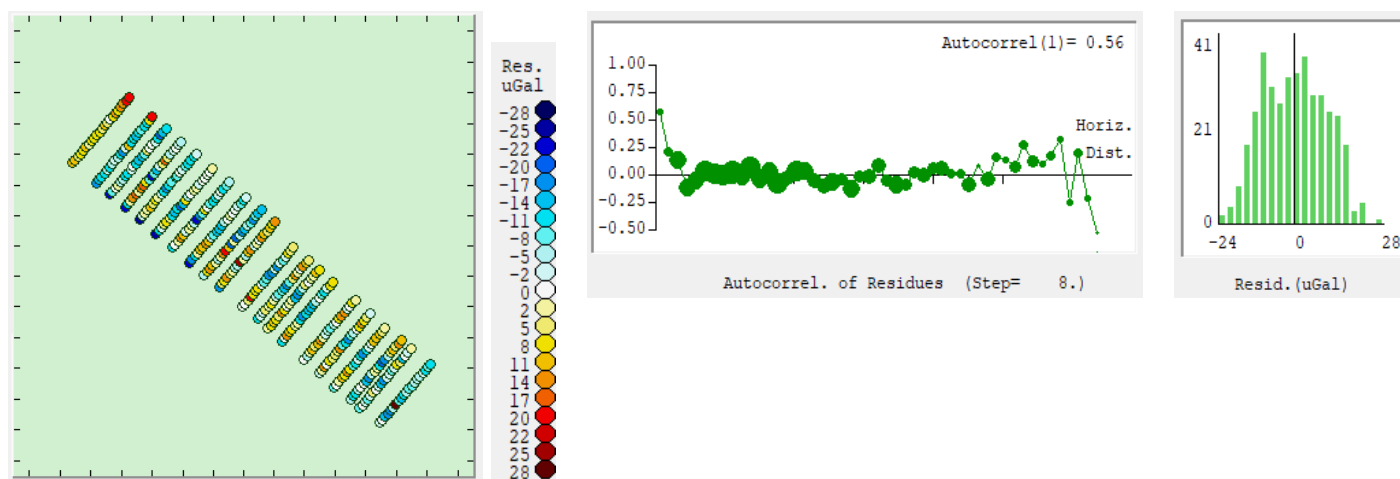


Figure B4

A tight-fit ($\lambda=50$) homogenous model ($\Delta\rho = -300 \text{ kg/m}^3$) with no trend co-adjustment, no residual reweighting ($B = 8$), and no depth weighting ($D = 0$). (a) top view (az. = 0, el. = 90), (b) 3D view from roughly NE (az. = 100, el. = 40), (c) lateral view from NE (az. = 135, el. = 0). Bold black lines represent access corridors. Inset in (a) is top view from Growth running screen.



This solution has tight fit (misfit: rms = 10 μGal , max = 28 μGal)

This solution has tight fit. This solution is similar to that of [figure B3](#). Now there is a little less expression of the shallow cavities associated with the corridors.

In [figure B5](#) we present a homogenous solution with $\Delta\rho = -300 \text{ kg/m}^3$, $\lambda = 70$, no trend co-adjustment, no reweighting of residuals ($B = 8$), and no depth weighting ($D = 0$). This solution is an adequate fit compact solution (misfit: rms = 15 μGal , max = 42 μGal).

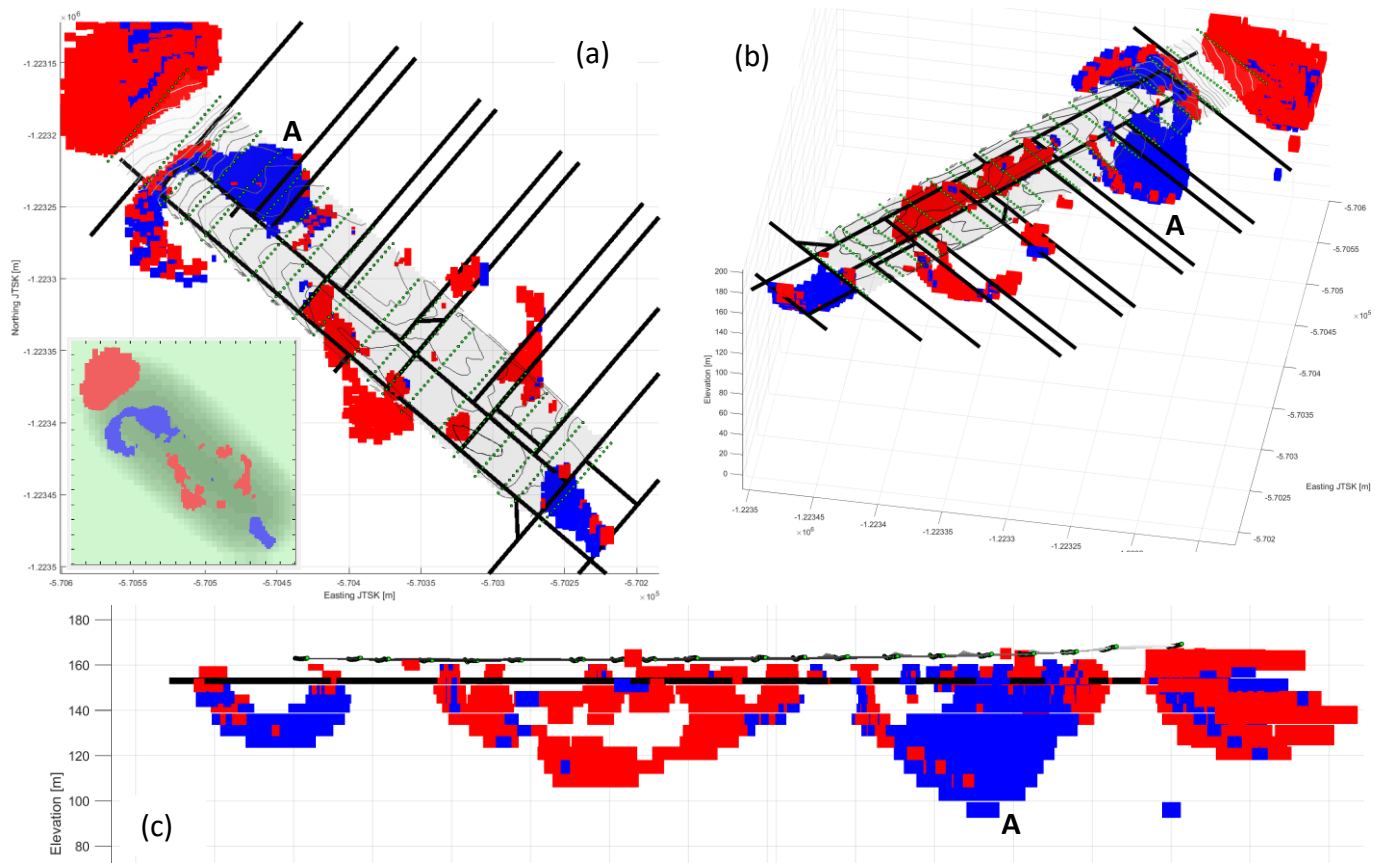
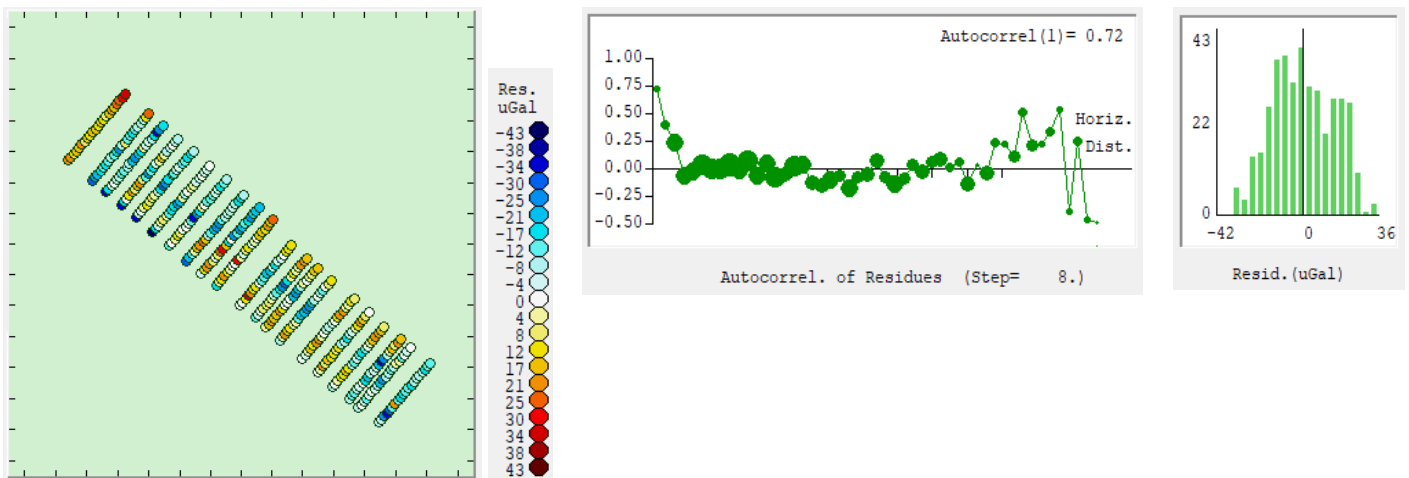


Figure B5

A compact ($\lambda = 70$) homogeneous model ($\Delta\rho = -300 \text{ kg/m}^3$) with no trend co-adjustment, no residual reweighting ($B = 8$), and no depth weighting ($D = 0$). (a) top view (az. = 0, el. = 90), (b) 3D view from roughly NE (az. = 100, el. = 40), (c) lateral view from NE (az. = 135, el. = 0). Bold black lines represent access corridors. Inset in (a) is top view from Growth running screen.



This solution has adequate fit (misfit: rms = 15 μGal , max = 42 μGal)

This solution is compact due to its adequate fit. This solution basically contains only information about the deep source body “A” and its neighboring (connected) negative contrast source bodies at the NW end of the data area. As this body cannot be interpreted as void space or back-filled space, the only left-over option is to interpret it as a geological source of negative density contrast. However, such working hypothesis is to be verified yet.

We have not run inversions with iterative residuals reweighting, as the data do not indicate any presence of outliers or bad data, and the data are well spatially correlated. For inversions with enabled depth weighting functionality, we used the GROWTH-23 tool and its upward-forcing feature. With the upward forcing functionality we are going to focus on the deep source body “A”. We will investigate the possibility of this being an expression of a surficial (surface-bound) flat body, interpreted in (Zahorec et al., 2021) as a back-filled surface collapse.

Next, we investigate heterogenous solutions with a **density contrast around 300 kg/m^3** , aimed at **seeking geological sources, partly collapsed/filled cavities, or surface collapses filled with tailings**, applying GROWTH-23. We used an average cell size of 8 m (suggested default value was 8.3 m). Growth suggested the default value for the balance factor $\lambda = 100$, which produced correct fit and solutions thus considered compact. By trial-and-error process we varied the end condition (%) to arrive at the final average density contrast of about 300 kg/m^3 . Again, the engagement of trend co-adjustment had virtually no impact on the solutions. Hence, we present solutions with no trend co-adjustment. Again, as in case of homogenous solutions, we applied no residuals reweighting, for the same reasons. We applied no flattening ($F = 0$), as no significant depth-ward density increase was expected. We focus on the impact of the upward-forcing functionality on the Growth solution.

In [figure B6](#) we present a heterogenous solution with $\% = 5$ (average $\Delta\rho = -280 \text{ kg/m}^3$, $\Delta\rho$ at 4 positive and negative values), $\lambda = 100$, no trend co-adjustment, no reweighting of residuals ($B = 8$), no flattening, and **no depth weighting** aka “upward forcing” ($D = 0$). This solution is an adequate fit compact solution.

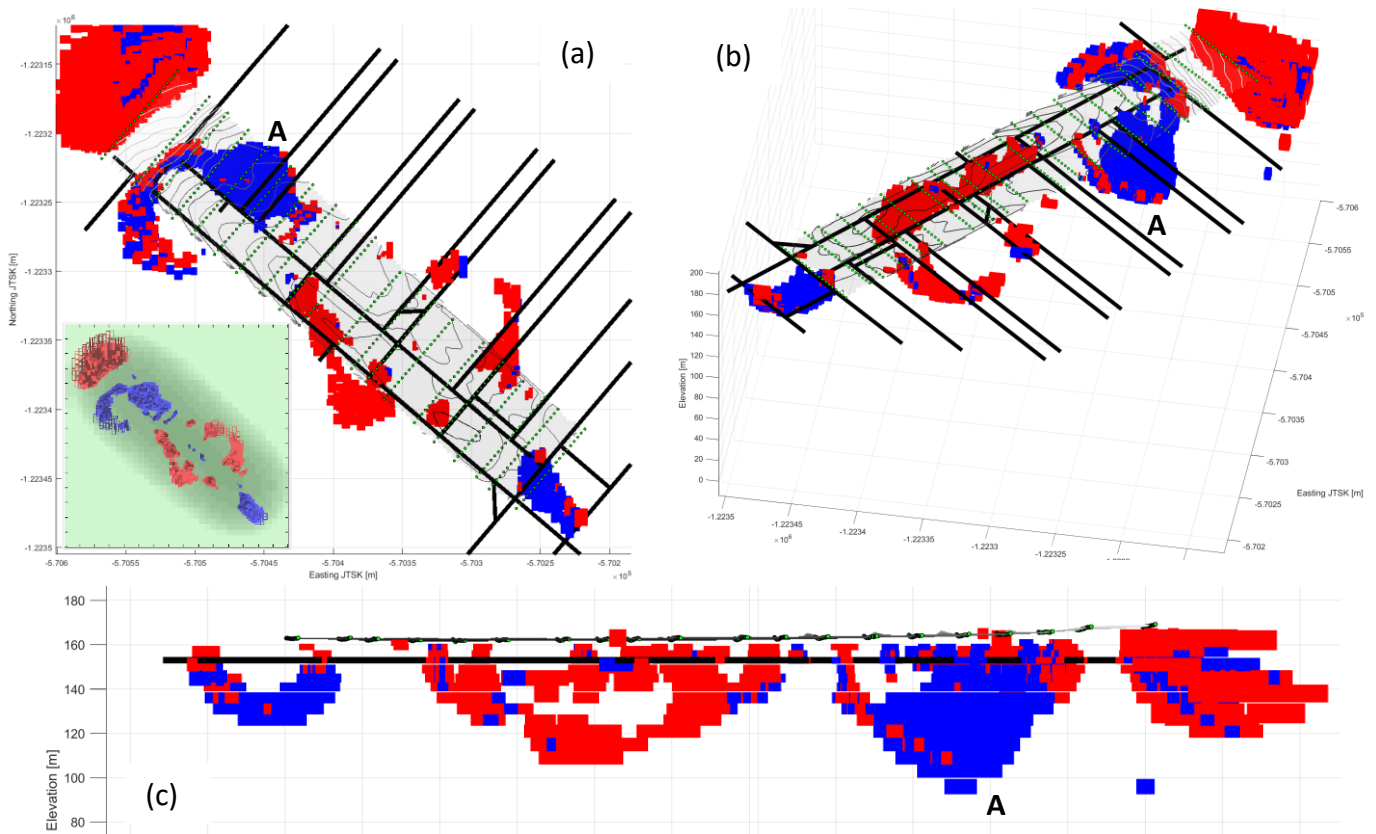
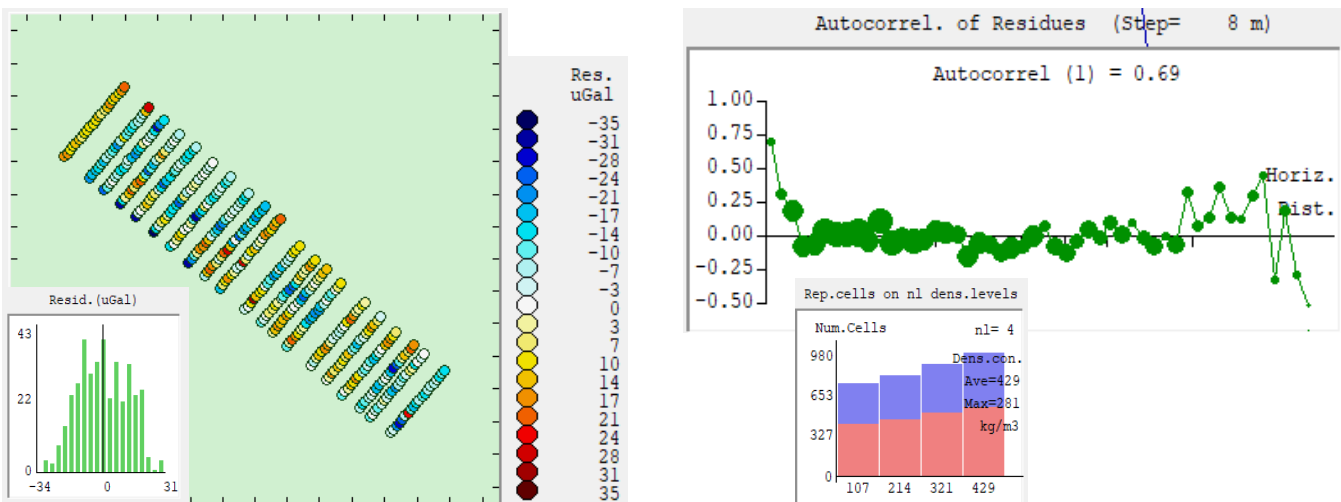


Figure B6

A compact ($\lambda = 100$) heterogenous model (av. $\Delta\rho = -280 \text{ kg/m}^3$) with no trend co-adjustment, no flattening, no residual reweighting ($B = 8$), and no depth weighting ($D = 0$). (a) top view (az. = 0, el. = 90), (b) 3D view from roughly NE (az. = 100, el. = 40), (c) lateral view from NE (az. = 135, el. = 0). Bold black lines represent access corridors. Inset in (a) is top view from Growth running screen.



This solution has adequate fit (misfit: rms = 13 μGal , max = 34 μGal)

This compact heterogenous solution is very similar to the compact homogenous solution of [figure B5](#).

In [figure B7](#) we present a heterogenous solution with $\% = 5$ (average $\Delta\rho = -267 \text{ kg/m}^3$, $\Delta\rho$ at 4 positive and negative values), $\lambda = 100$, no trend co-adjustment, no reweighting of residuals ($B = 8$), no flattening, and **weak depth weighting** aka “upward forcing” ($D = 5$). This solution is an adequate fit compact solution.

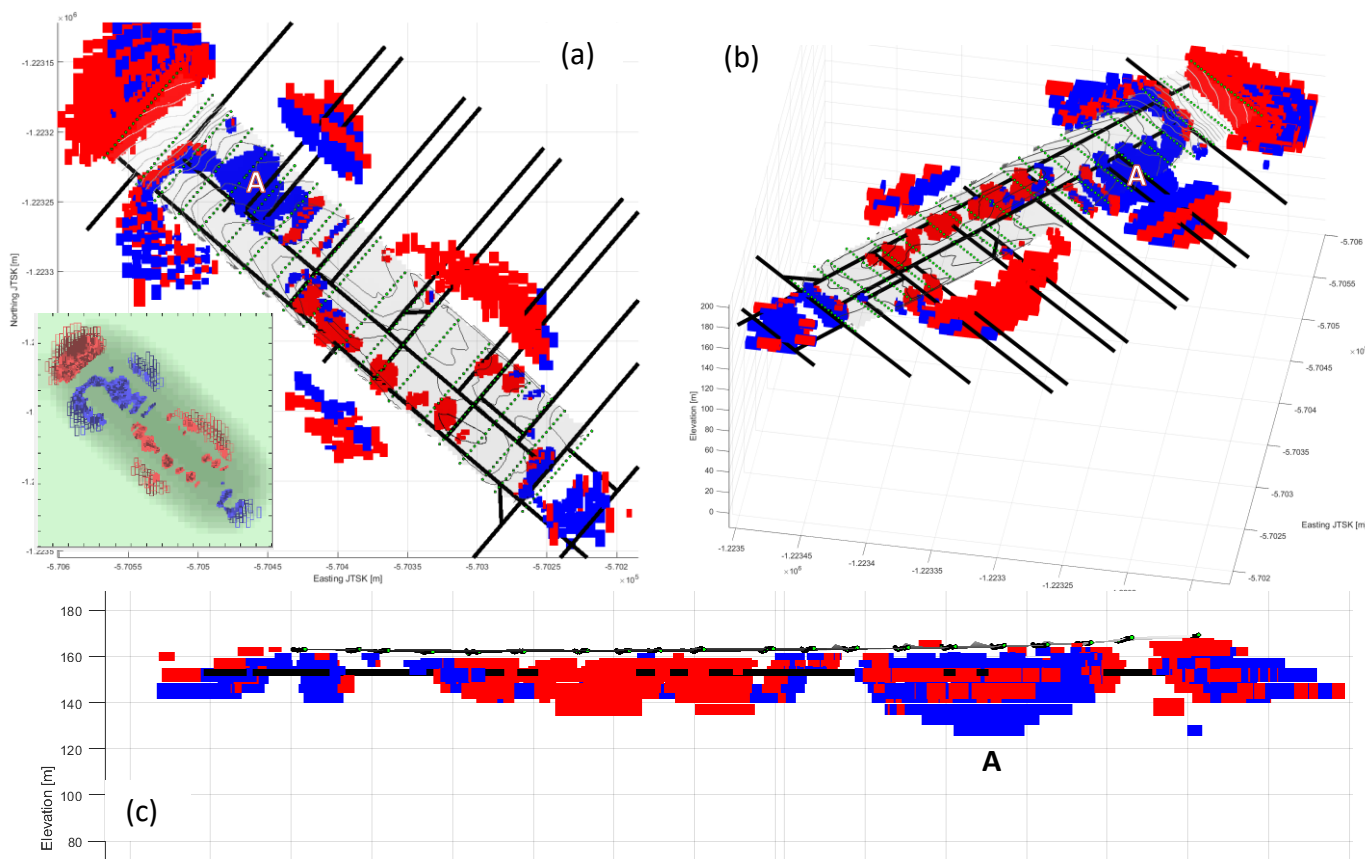
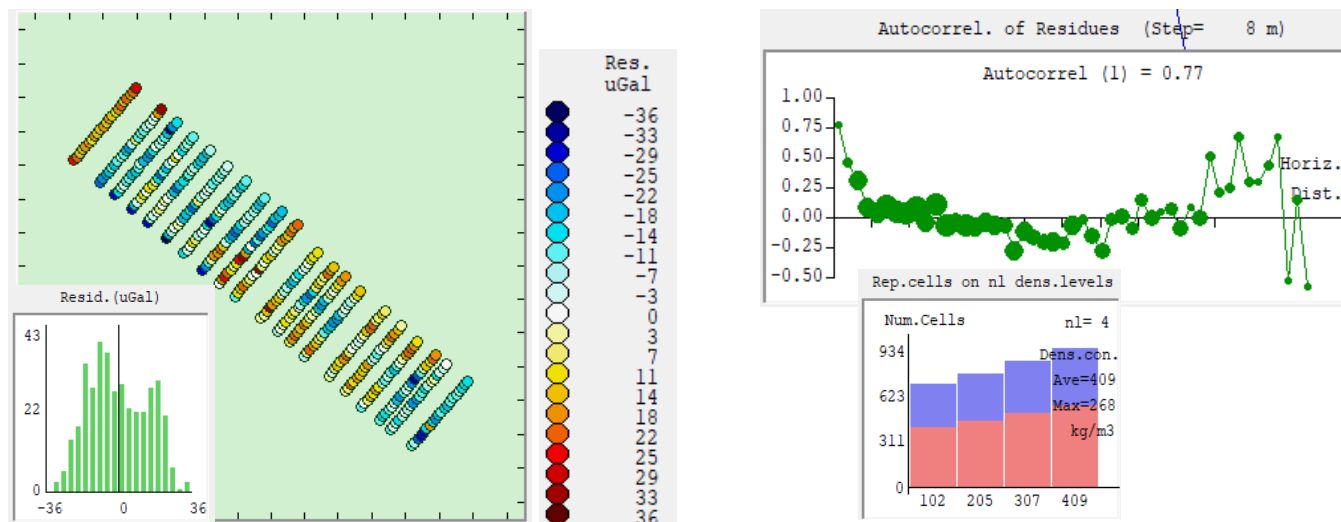


Figure B7

A compact ($\lambda = 100$) heterogenous model (av. $\Delta\rho = -267 \text{ kg/m}^3$) with no trend co-adjustment, no flattening, no residual reweighting ($B = 8$), and **weak depth weighting** ($D = 5$). (a) top view (az. = 0, el. = 90), (b) 3D view from roughly NE (az. = 100, el. = 40), (c) lateral view from NE (az. = 135, el. = 0). Bold black lines represent access corridors. Inset in (a) is top view from Growth running screen.



This solution has adequate fit (misfit: rms = 15 μGal , max = 36 μGal)

The deep source body “A” is in this solution with weak upward forcing shallower than that in the solution of [figure B6](#). It spans vertically from a couple of meters below surface to about 35 m below surface. Notice that due to the engaged upward forcing the autocorrelation function starts getting worse and the Gaussian distribution of residuals is slightly disturbed also.

In [figure B8](#) we present a heterogenous solution with $\% = 4$ (average $\Delta\rho = -303 \text{ kg/m}^3$, $\Delta\rho$ at 4 positive and negative values), $\lambda = 100$, no trend co-adjustment, no reweighting of residuals ($B = 8$), no flattening, and **moderate depth weighting** aka “upward forcing” ($D = 10$). This solution is an adequate fit compact solution.

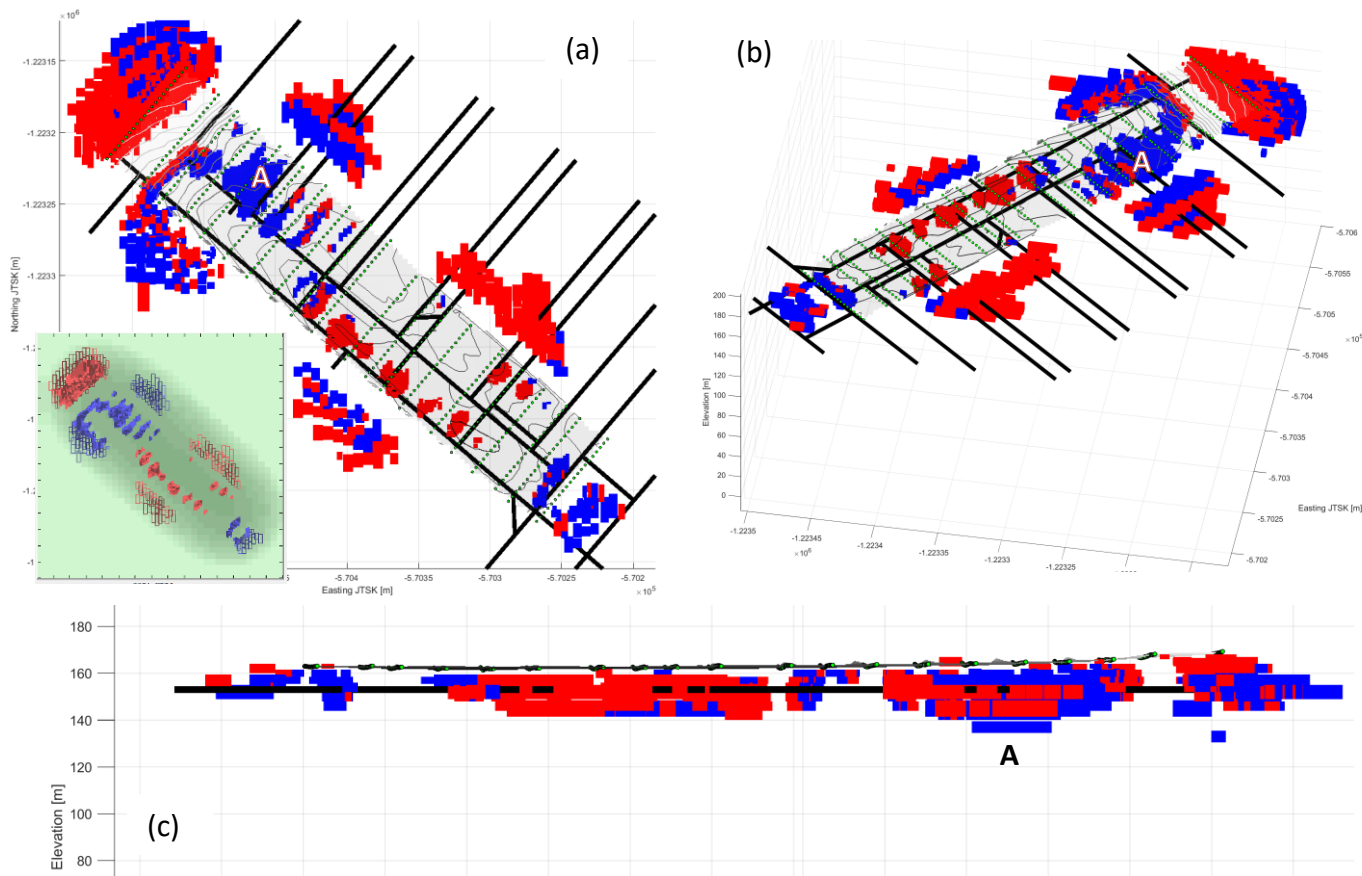
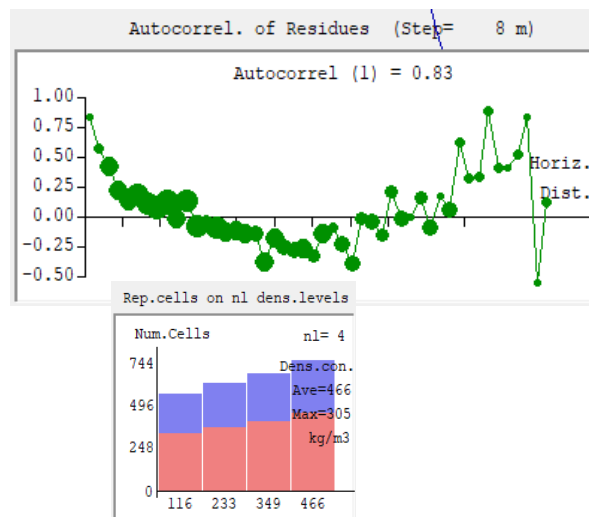
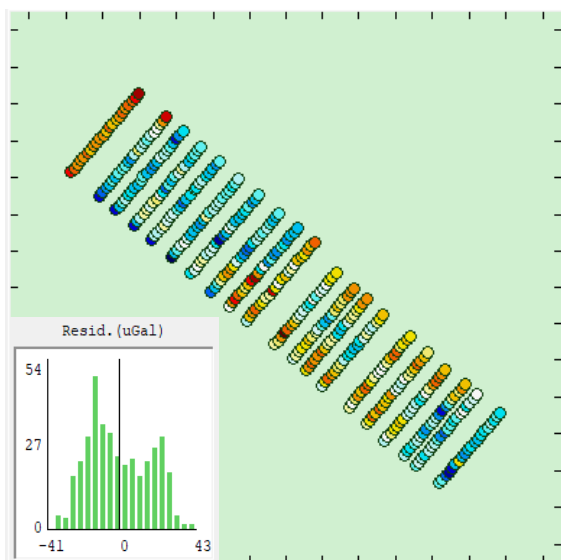


Figure B8

A compact ($\lambda = 100$) heterogenous model (av. $\Delta\rho = -303 \text{ kg/m}^3$) with no trend co-adjustment, no flattening, no residual reweighting ($B = 8$), and **moderate depth weighting** ($D = 10$). (a) top view (az. = 0, el. = 90), (b) 3D view from roughly NE (az. = 100, el. = 40), (c) lateral view from NE (az. = 135, el. = 0). Bold black lines represent access corridors. Inset in (a) is top view from Growth running screen.



This solution has fair fit (misfit: rms = 18 μGal , max = 43 μGal)

The deep source body “A” is in this solution with moderate upward forcing shallower than that in the solution of [figure B7](#). It spans vertically from a couple of meters below surface to about 28 m below surface. Due to the engaged moderate upward forcing the autocorrelation function is still worse and the Gaussian distribution of residuals is disturbed even more. A pattern of artifacts parallel with the SW–NE trending data profiles becomes dominant.

In figure B9 we present a heterogenous solution with $\% = 4$ (average $\Delta\rho = -296 \text{ kg/m}^3$, $\Delta\rho$ at 4 positive and negative values), $\lambda = 100$, no trend co-adjustment, no reweighting of residuals ($B = 8$), no flattening, and **strong depth weighting** aka “upward forcing” ($D = 30$). This solution is a slightly poorer-fit compact solution.

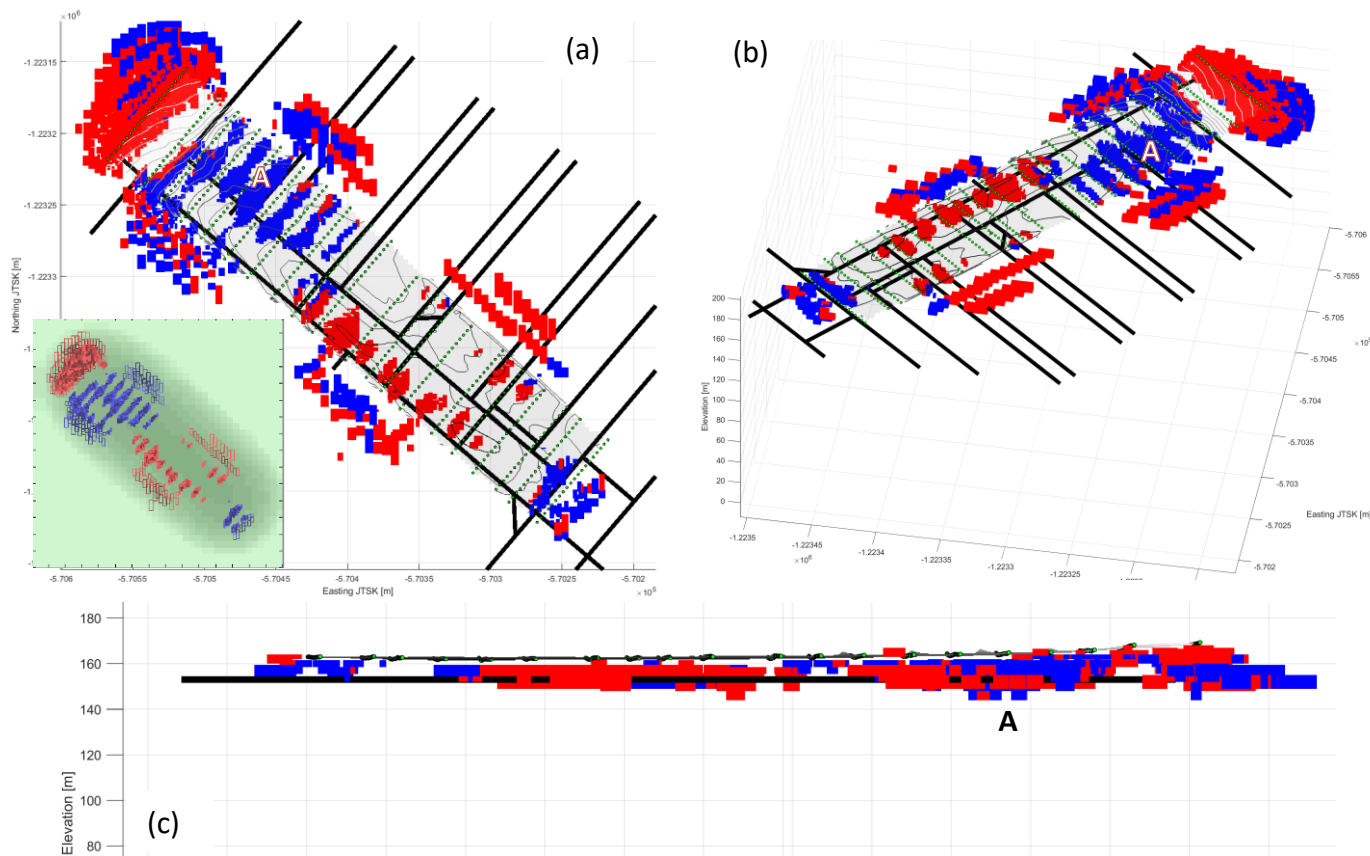
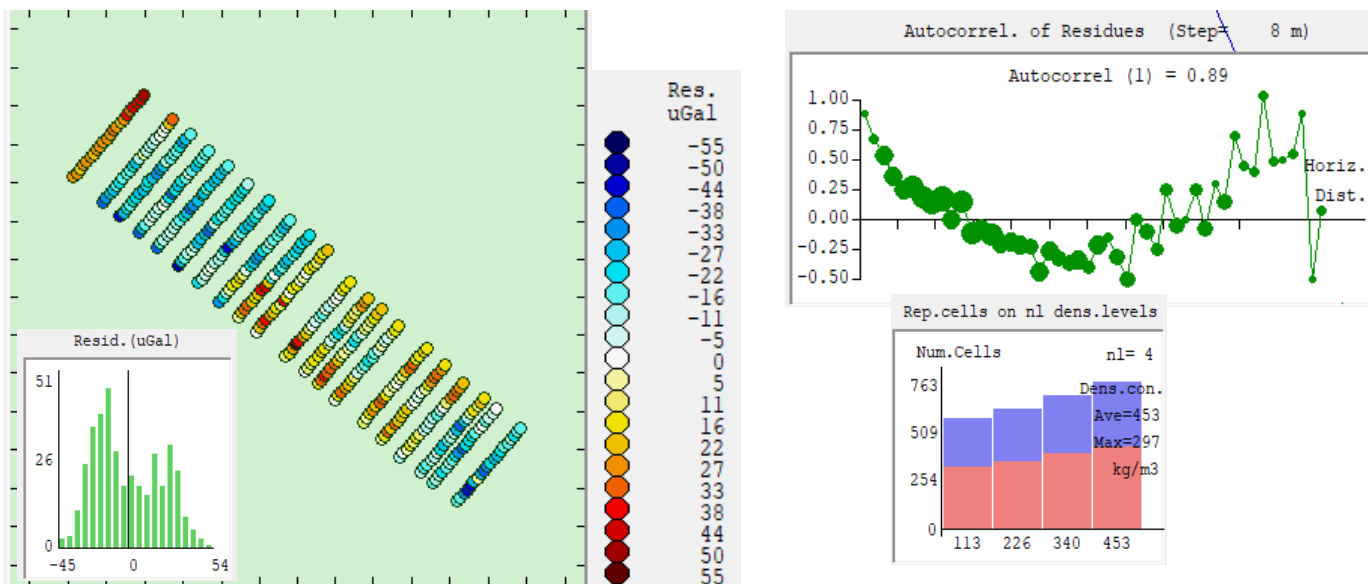


Figure B9

A compact ($\lambda = 100$) heterogenous model (av. $\Delta\rho = -296 \text{ kg/m}^3$) with no trend co-adjustment, no flattening, no residuals reweighting ($B = 8$), and **strong depth weighting** ($D = 30$): (a) top view (az. = 0, el. = 90), (b) 3D view from roughly NE (az. = 100, el. = 40), (c) lateral view from NE (az. = 135, el. = 0). Bold black lines represent access corridors. Inset in (a) is top view from Growth running screen.



This solution has a poorer fit (misfit: rms = 22 μGal , max = 54 μGal)

This solution with strong upward forcing breaks up completely into shallow artifacts placed in-between the data profiles and parallel to them. Even now, the depth-reach of the artifacts related to source body “A” does not get above the horizon of the corridors. This challenges the possibility that the pronounced gravity low (“A”) is produced solely by a surficial flat thin body of a back-filled surface depression due to surface subsidence.

Additional heterogenous (GROWTH-23) solutions
presented as Growth run screens, horizontal model slices and W-E vertical model sections

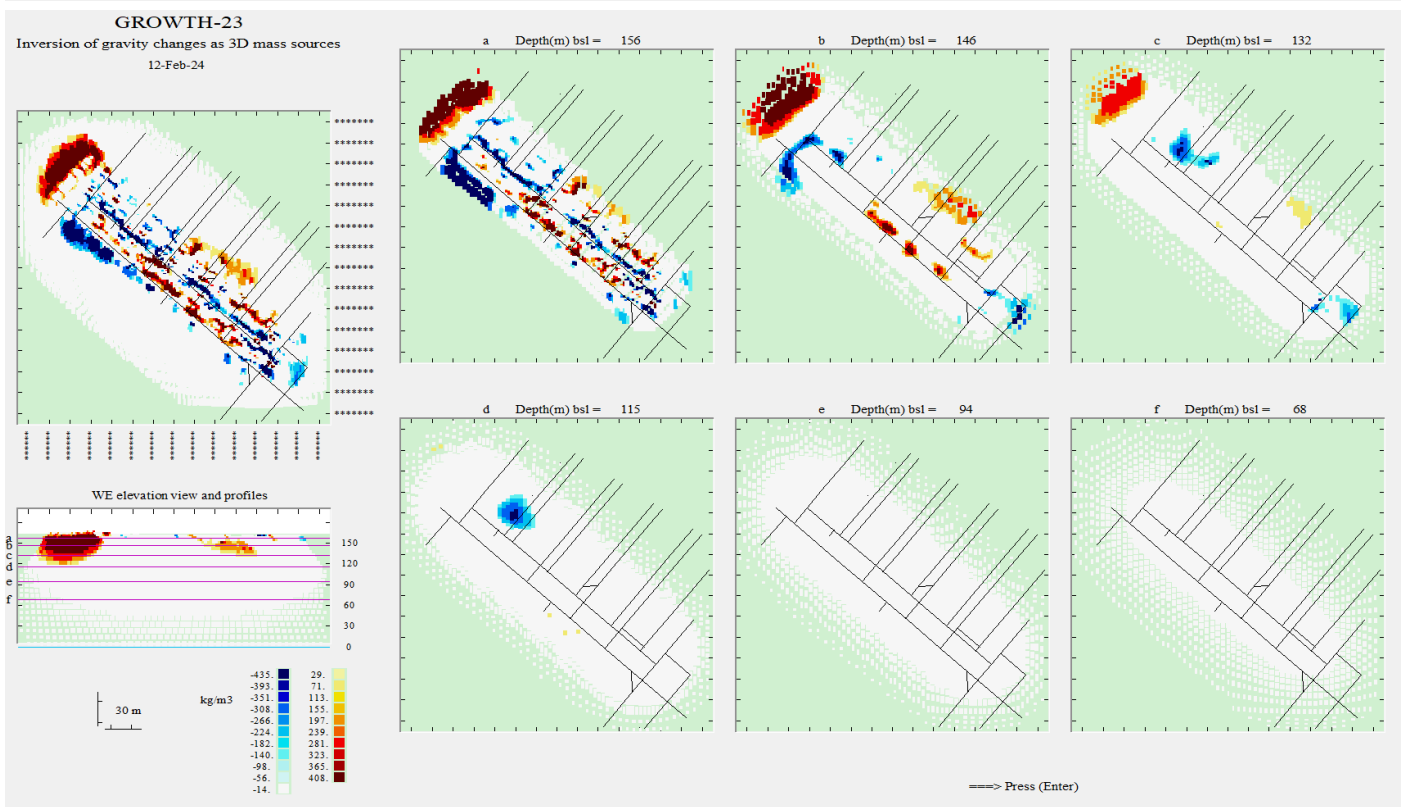
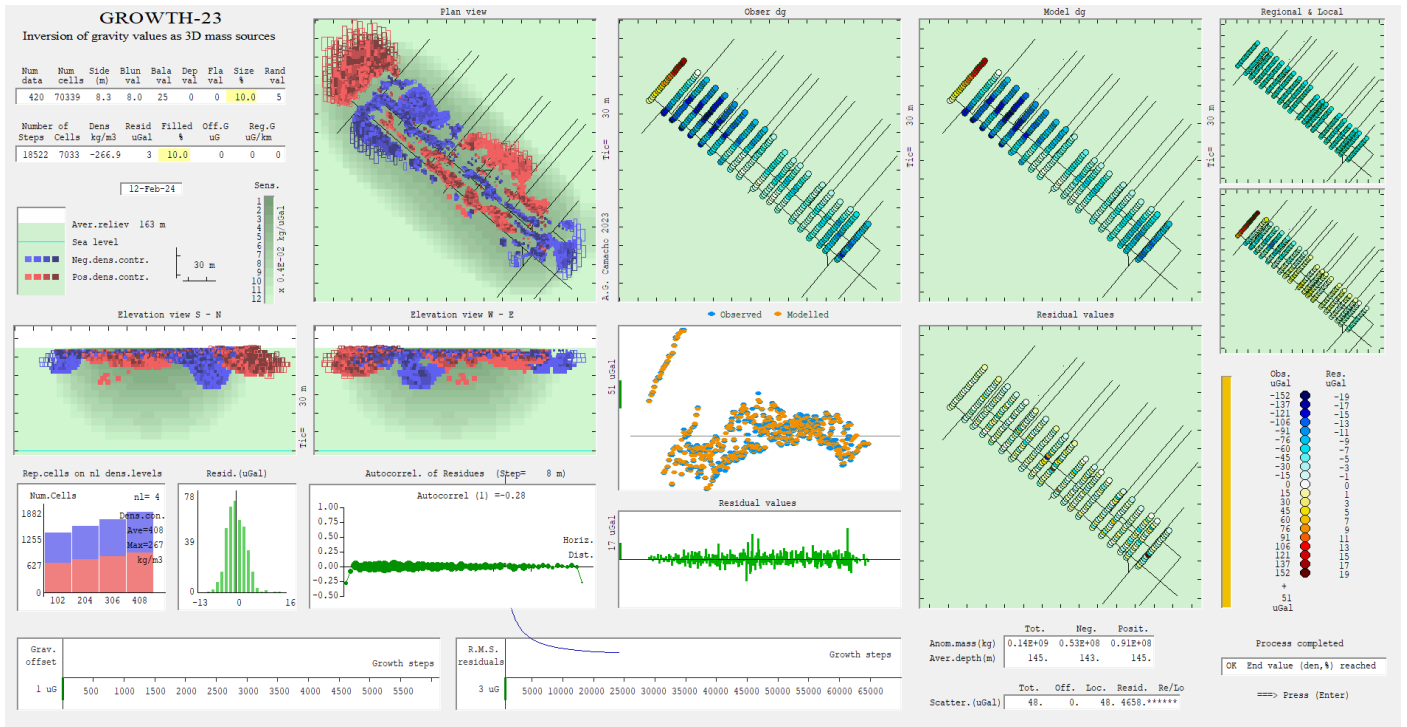


Figure C1 (continued below)

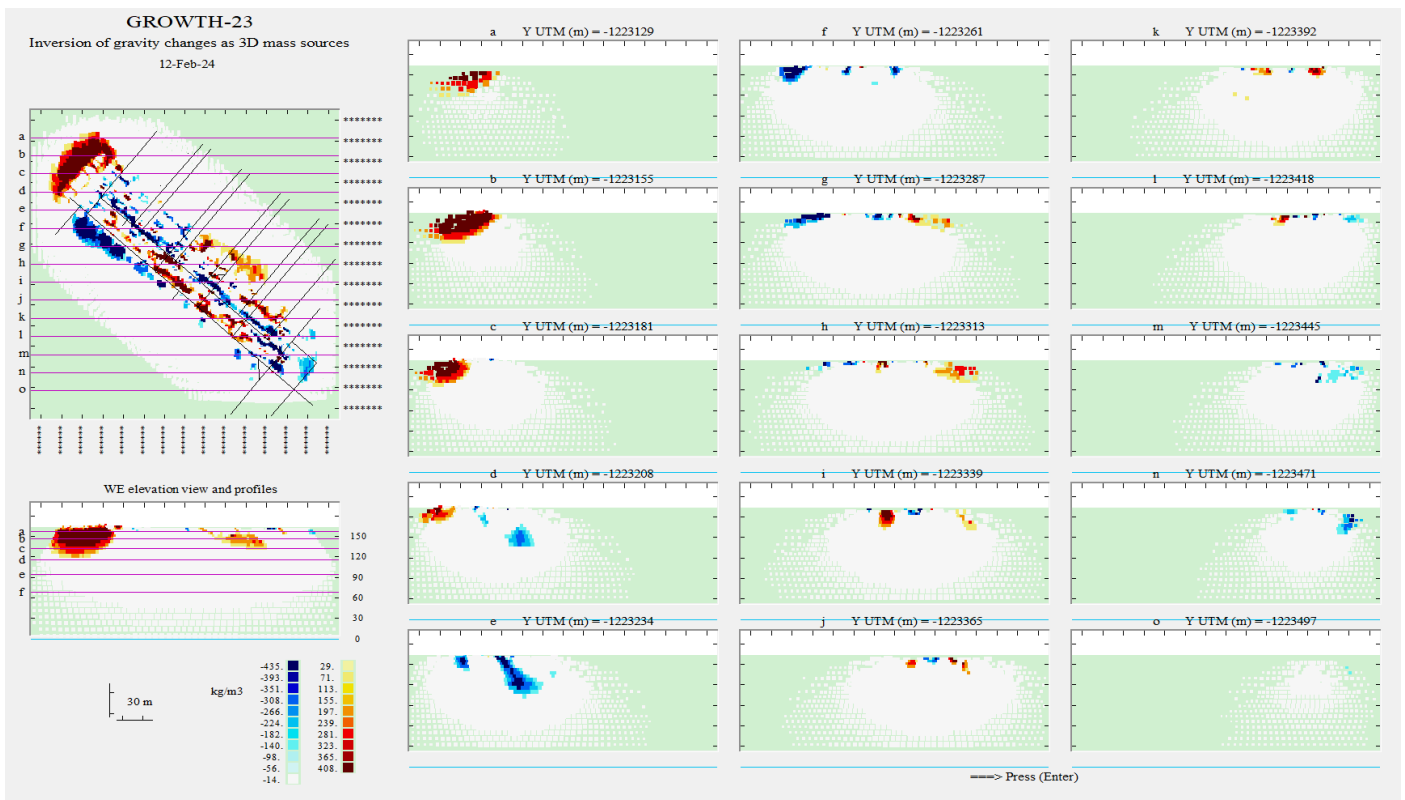


Figure C1

An overfitting Growth solution ($\lambda = 25$, % = 10, average $\Delta\rho = -267 \text{ kg/m}^3$, no residuals reweighting, no flattening, no depth weighting) with misfit r.m.s. = $3 \mu\text{Gal}$, max = $13 \mu\text{Gal}$. Growth running screen with top and lateral views at the 3D model (top), horizontal slices at various depths (middle), and various W–E vertical sections (bottom).

Although this solution is overfitting and thus may be polluted by artefacts, it offers valuable information. Clearly, this solution captures the linearly aligned (parallel with corridors) mostly connected negative density contrast small bodies at the depth of about 7 m below surface (slice (a) in the middle plot, located at 156 m a.s.l., the surface being at roughly 163 m a.s.l.). All the corridors are roughly at 10 m below surface. In the same slice we see an interesting twin-alignment section, appearing as two shorter parallel lines in the NW sector, running parallel with corridor 1, yet slightly offset from it towards SW. The one which is closer to corridor 1 seems to have a continuation in terms of sporadic yet perfectly lined-up negative spots also in the SE sector, with the same offset, indicated by five negative contrast spots (small point-wise sources).

What is intriguing is the appearance of a deep source in this overfitting Growth solution, seen in slices (c) 31 m below surface and (d) 48 m below surface. In W–E vertical sections it is seen in section (e) and partly in (d). It reaches depths of about 55 m below surface. It creeps downward from the level of the access corridors at a slanted angle. Horizontal slice (b) 17 m below surface captures its apparent transition from the corridors to deeper depths. There are no reasons to consider this source as artifact. However, its origin and nature remain a mystery for now, left for additional exploration.

In figure C2 we show a model with the same inversion parameters as in figure C1, this time with a relatively strong depth weighting, aka upward forcing ($D = 15$).

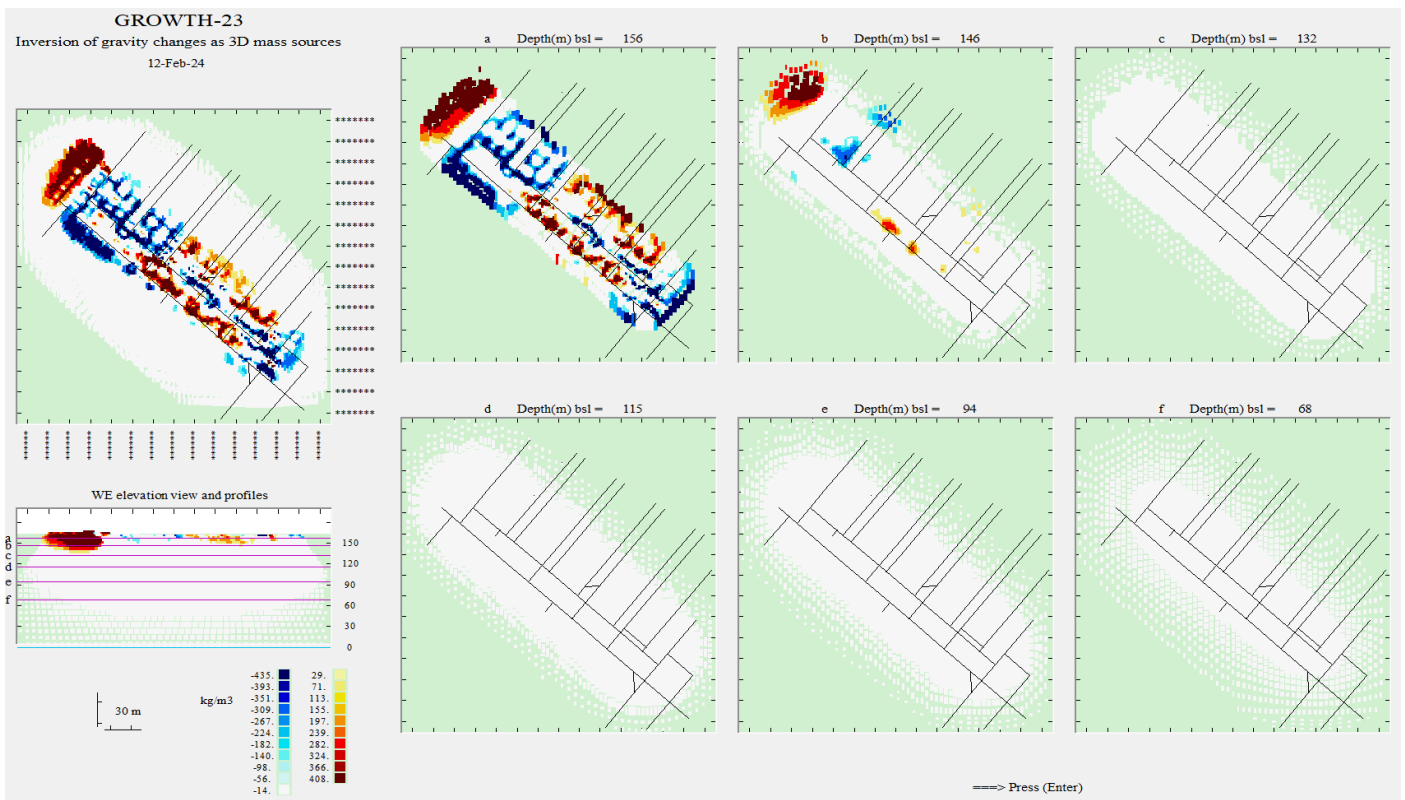
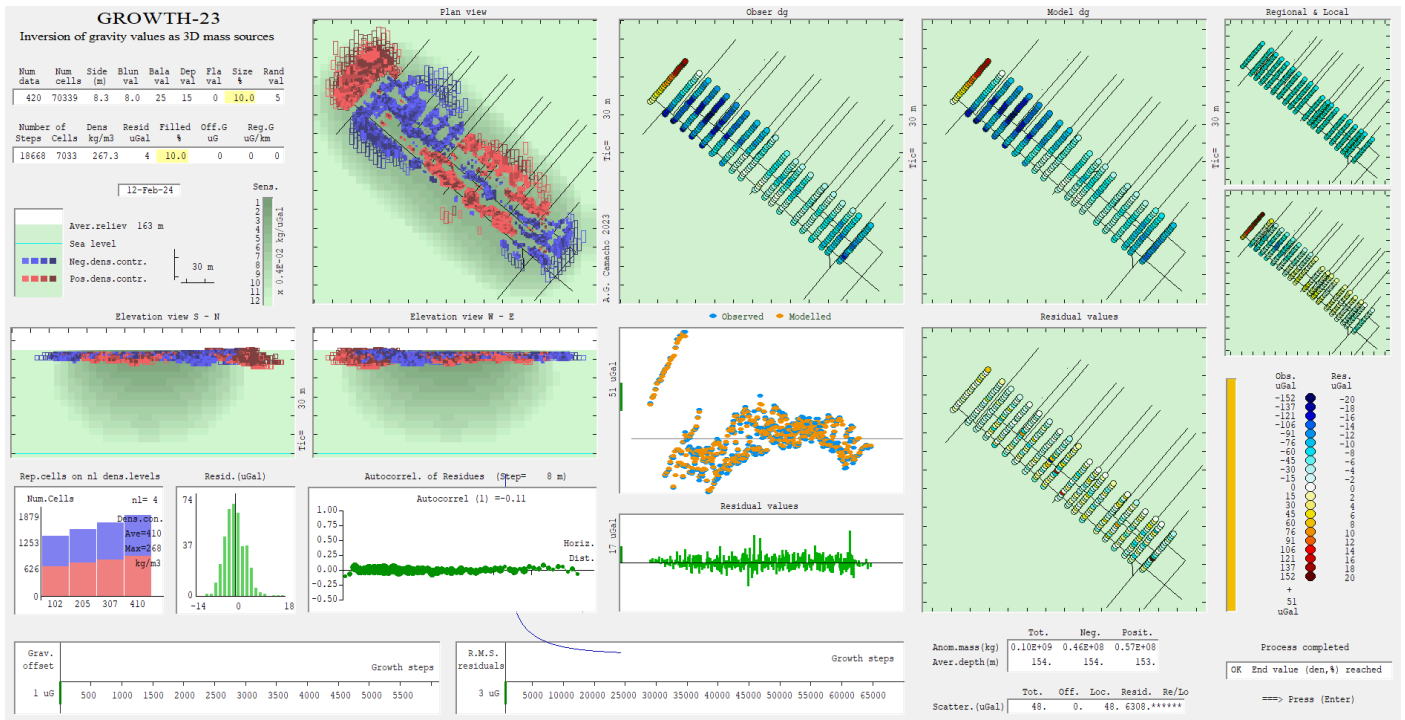


Figure C2 (continued below)

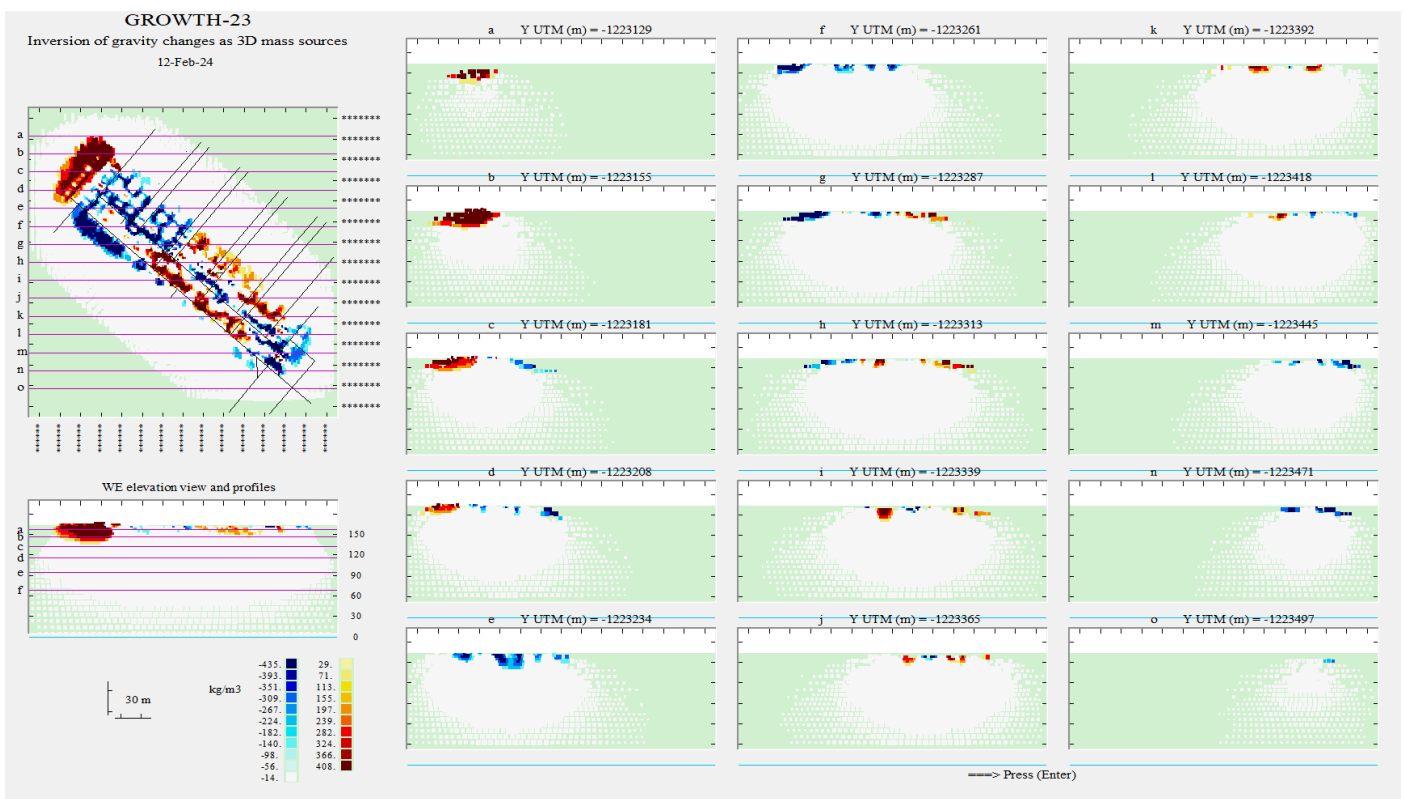


Figure C2

An overfitting Growth solution ($\lambda = 25$, $\% = 10$, average $\Delta\rho = -267 \text{ kg/m}^3$, no residuals reweighting, no flattening, strong depth weighting with $D = 15$) with misfit r.m.s. = $4 \mu\text{Gal}$, max = $14 \mu\text{Gal}$. Growth running screen with top and lateral views at the 3D model (top), horizontal slices at various depths (middle), and various W–E vertical sections (bottom).

The depth weighting (upward forcing) pushed the deep source upwards, squeezed it towards shallower depths. Now the deep source goes down only to about 20 m below surface, seen in slice (b) at 17 m below surface, and also in vertical section (e). Still, it is about 10 m below the horizon of the access corridors. So even with strong depth weighting the existence of the deep source remains an option. However, the depth weighting produces a lot of shallow sources (at the horizon of the access corridors), which appear to be “checkerboard” artifacts. The feature of depth weighting introduces another level of ambiguity into the Growth solutions. If there are reasons to apply depth weighting to obtain a more realistic solution, the correct value of the D parameter must be determined by a trial-and-error process, matching the Growth model to borehole data or other applicable independent structural information. Since at Čáry we lack such sort of information below the depth level of 30 m below surface, we favor solutions with no or very weak depth weighting.

The gravity data at Čáry is observed on profiles with relatively small step of 4 m, while the spacing between profiles is 20 m on average. The depth weighting, for this kind of input data, perhaps also with the combination of smaller λ values, generates pronounced artifacts aligned parallel with the data profiles. The stronger the depth weighting (the higher the D values), the more is the solution is polluted with artefacts.

Compact to over-compacted solutions

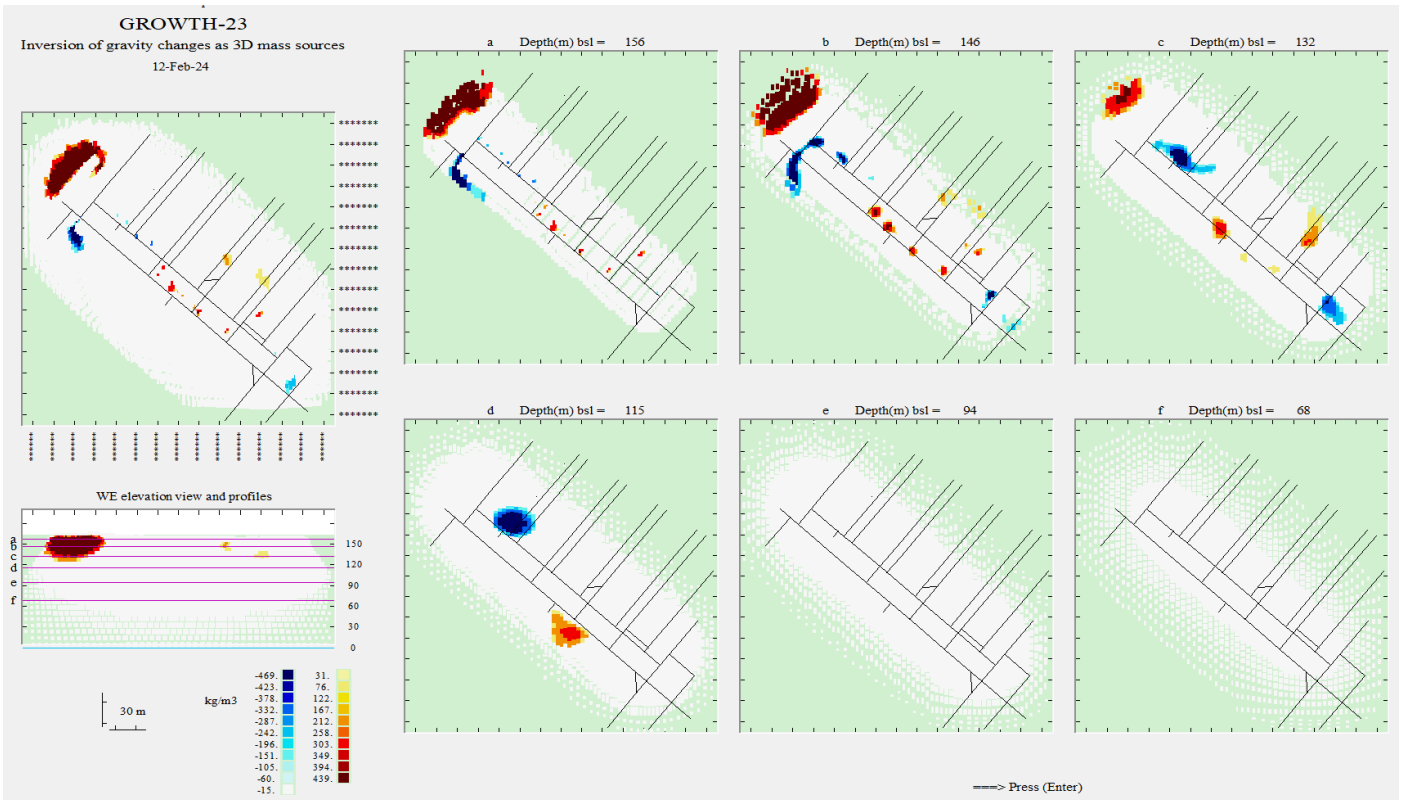
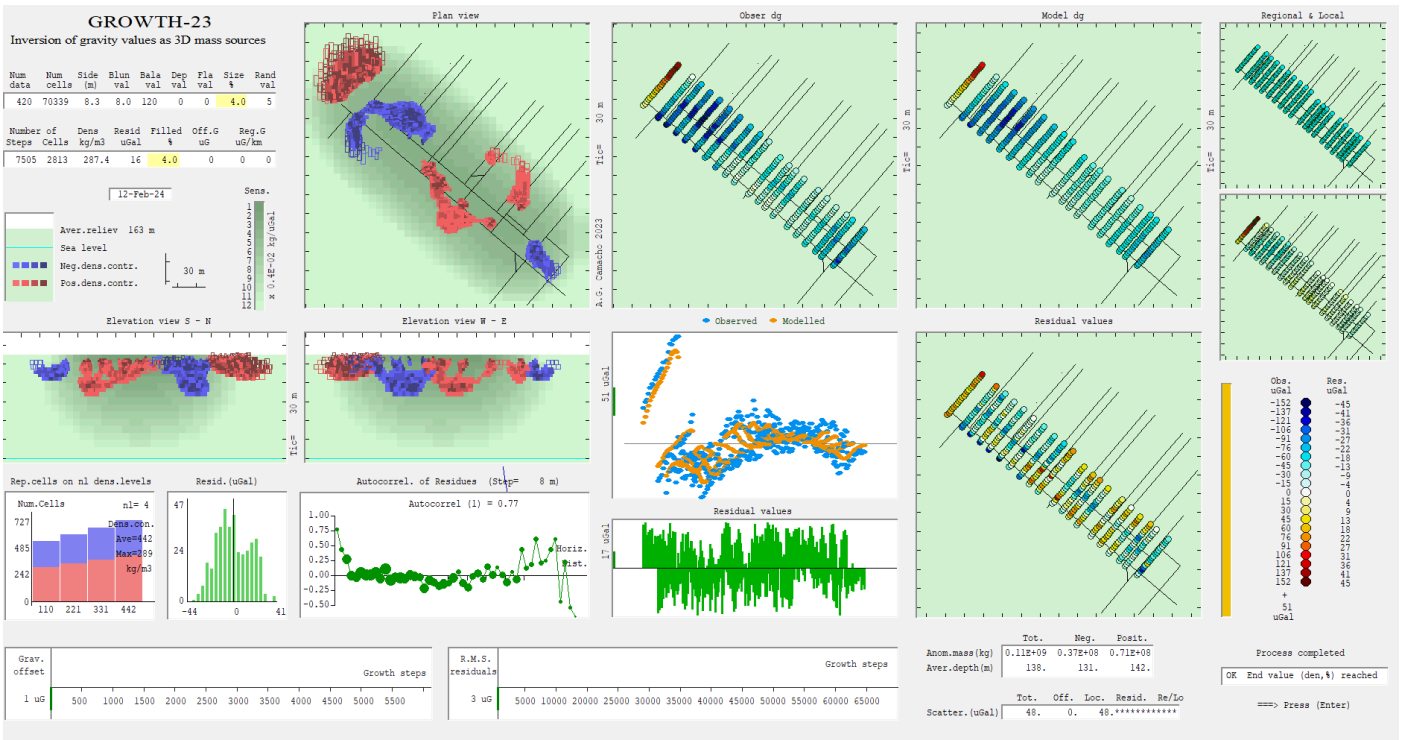


Figure C3 (continued below)

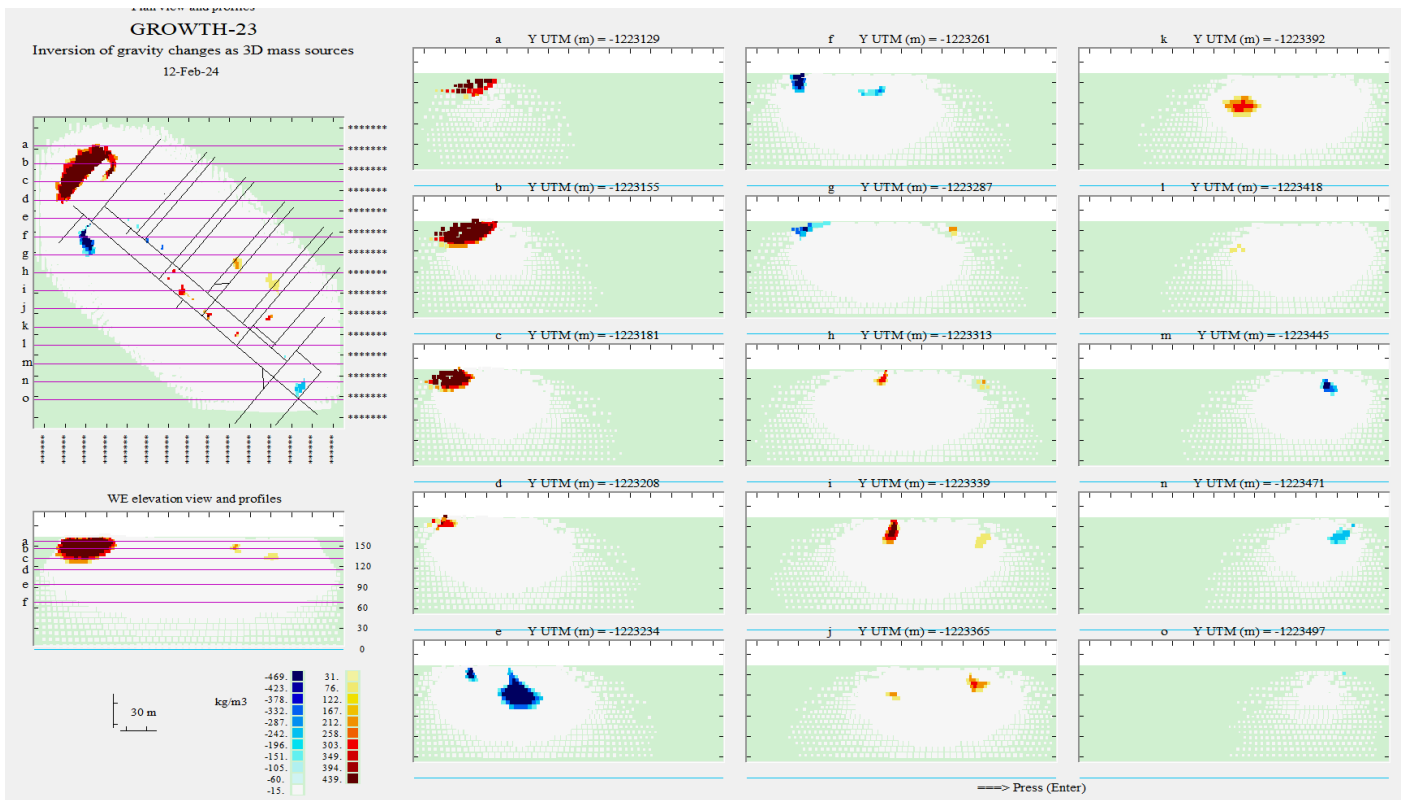


Figure C3

Slightly over-compacted Growth solution with poor data fit ($\lambda = 120$, % = 4, average $\Delta\rho = -287 \text{ kg/m}^3$, no residuals reweighting, no flattening, no depth weighting with $D = 0$, with misfit: r.m.s. = $16 \mu\text{Gal}$, max = $44 \mu\text{Gal}$). Growth running screen with top and lateral views at the 3D model (top), horizontal slices at various depths (middle), and various W–E vertical sections (bottom).

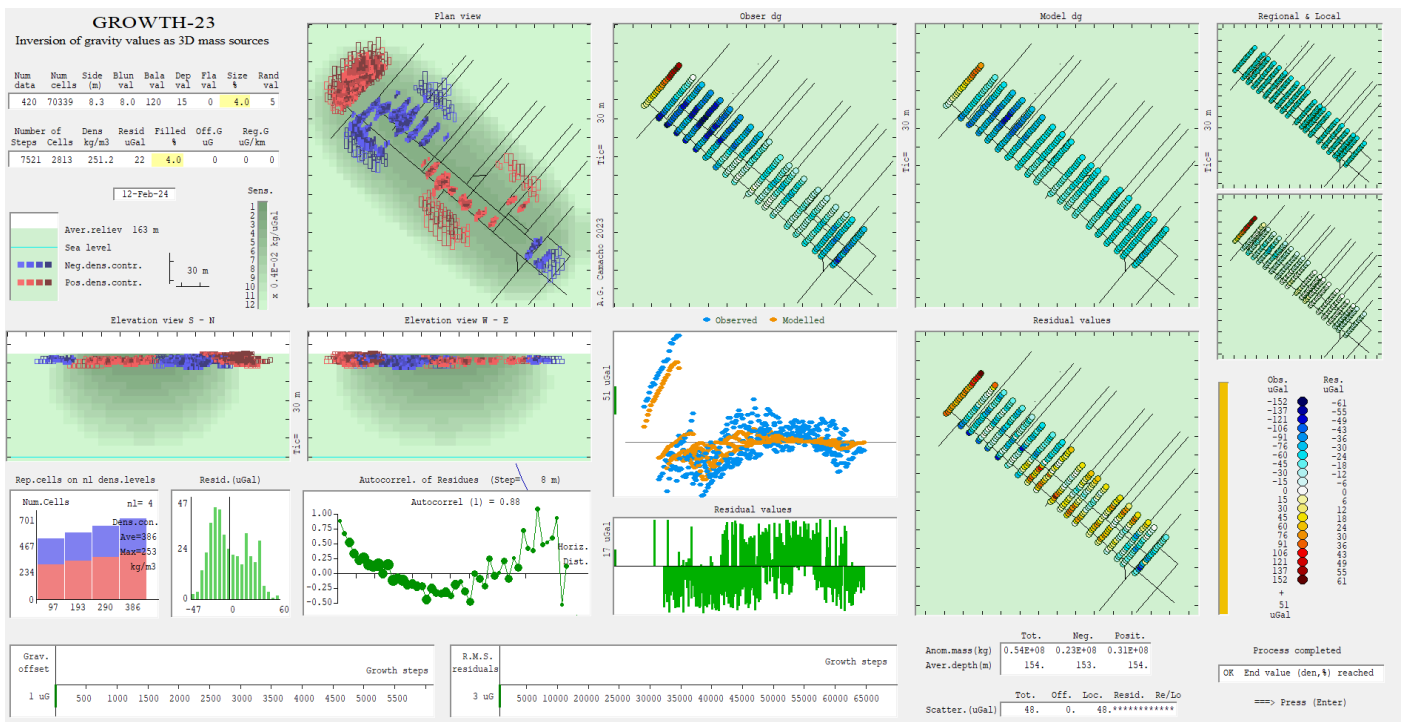


Figure C4 (continued below)

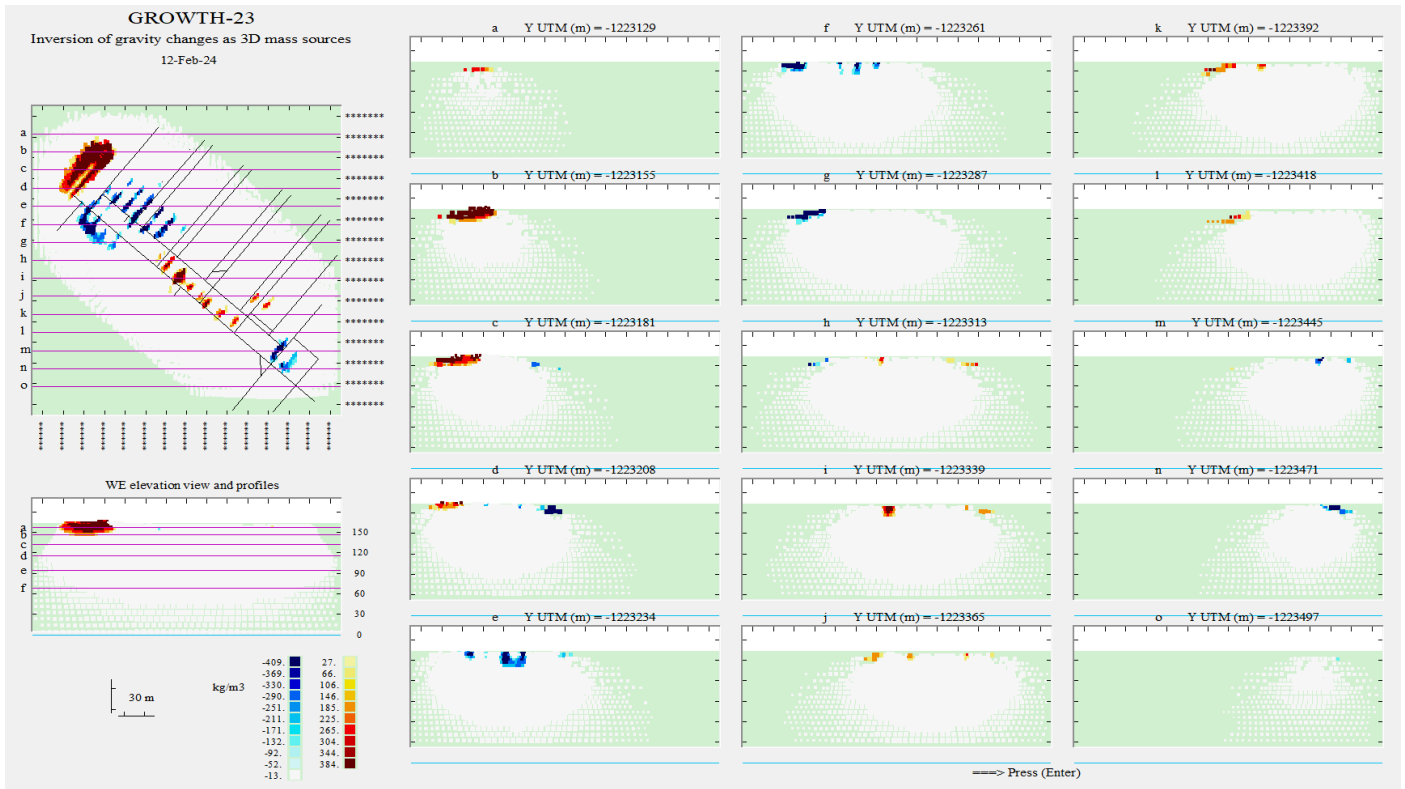
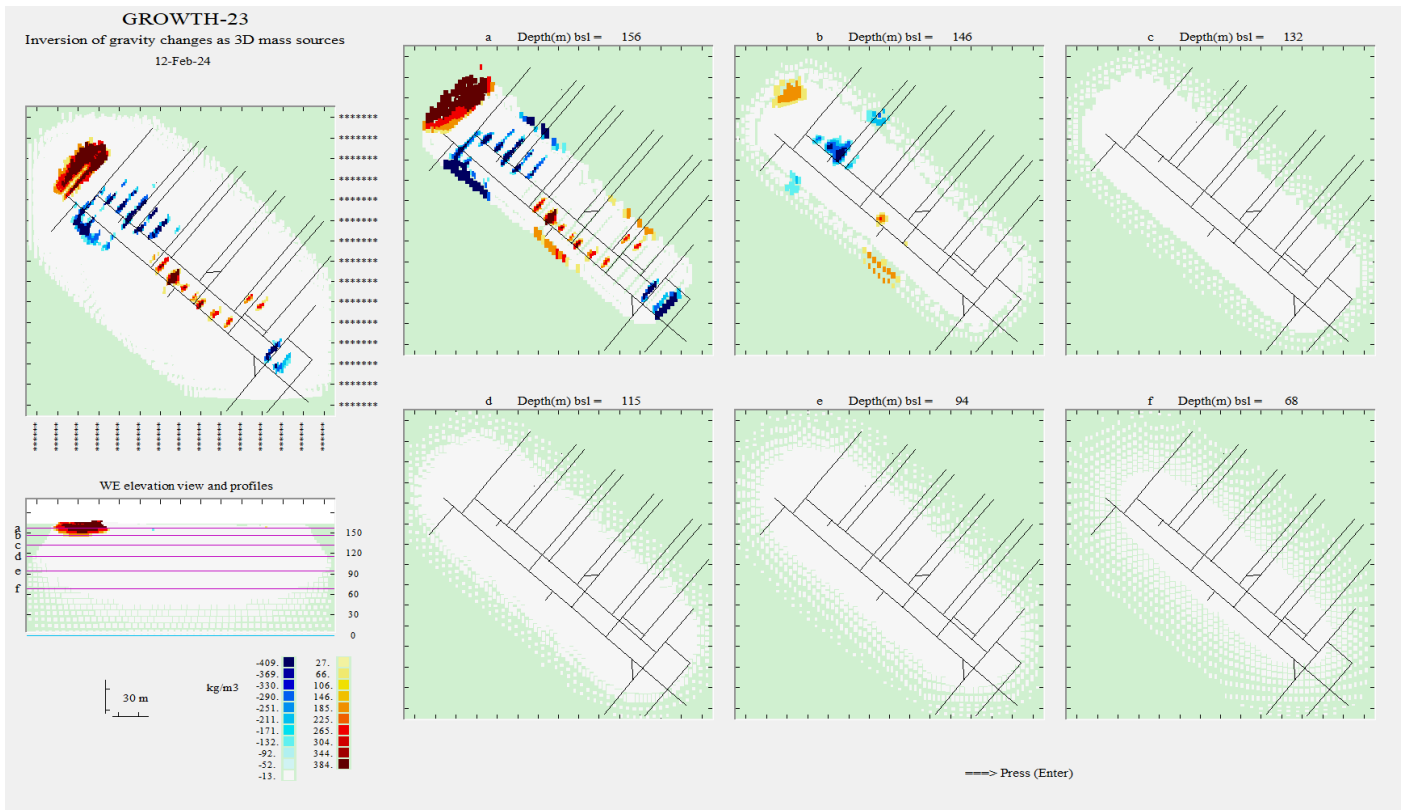


Figure C4

Over-compacted Growth solution with poor data fit ($\lambda = 120$, % = 4, average $\Delta\rho = -251 \text{ kg/m}^3$, no residuals reweighting, no flattening, this time with strong depth weighting with $D = 15$, with misfit: r.m.s. = $22 \mu\text{Gal}$, max = $60 \mu\text{Gal}$). Growth running screen with top and lateral views at the 3D model (top), horizontal slices at various depths (middle), and various W–E vertical sections (bottom).

No matter if overfitting or over-compacted solution, depth weighting produces strong shallow artificial sources at or in-between data profiles.

Focusing on the deep source (inversions for truncated data area over the gravity low)

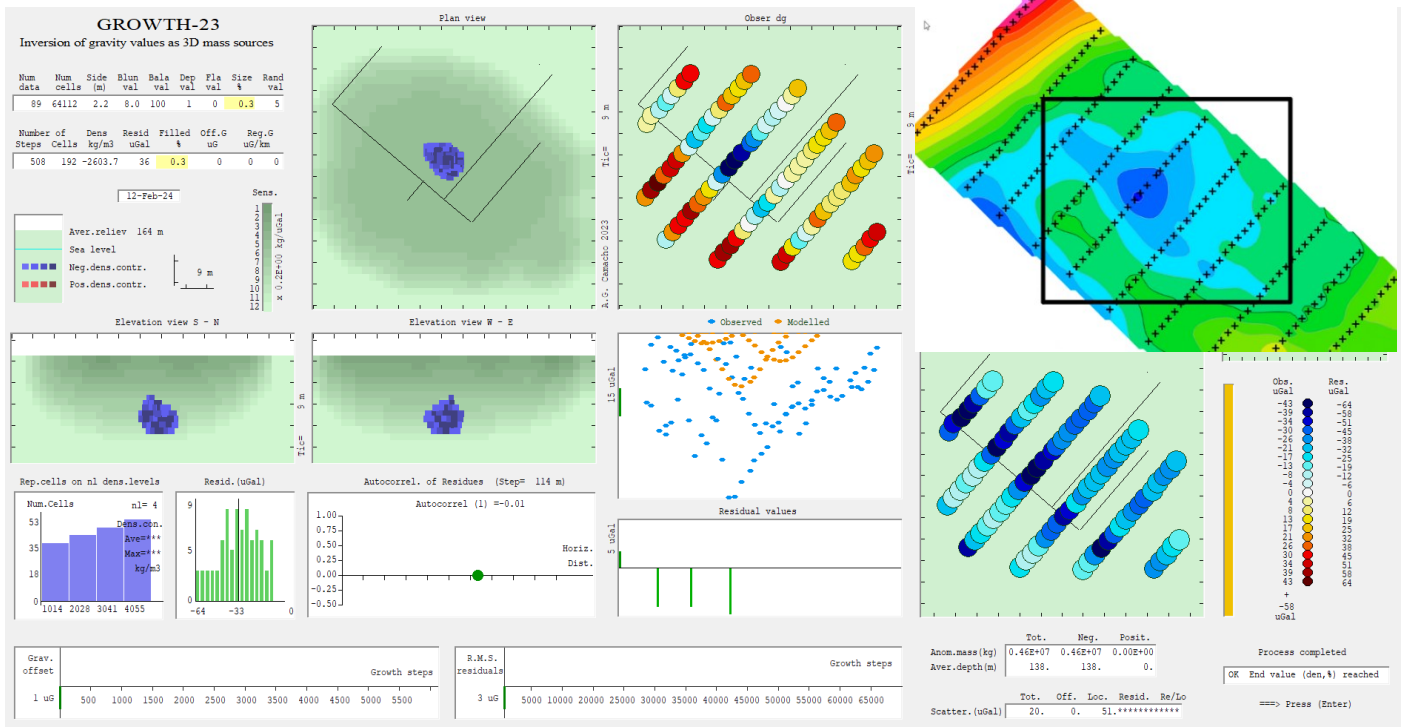


Figure C5

Over-compacted Growth solution with poor data fit and average density contrast roughly related to void space ($\lambda = 100$, % = 0.3, average $\Delta\rho = -2604 \text{ kg/m}^3$, no residuals reweighting, no flattening, weak depth weighting with $D = 1$, with misfit: r.m.s. = $36 \text{ } \mu\text{Gal}$, max = $64 \text{ } \mu\text{Gal}$). Growth running screen with top and lateral views at the 3D model. Tick mark is 9 m. The deep body is centered at about 25 m below surface.

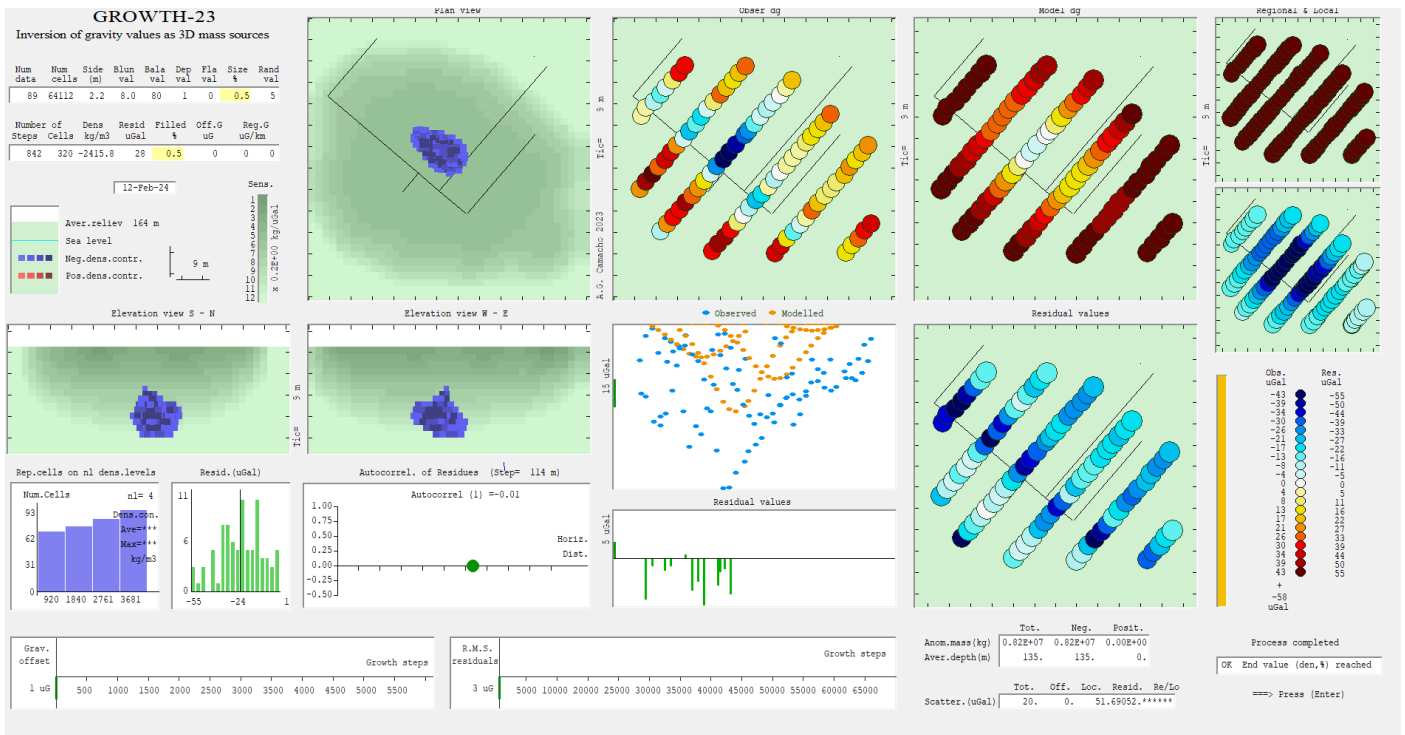


Figure C6

Over-compacted Growth solution with poor data fit and average density contrast roughly related to void space ($\lambda = 80$, % = 0.5, average $\Delta\rho = -2416 \text{ kg/m}^3$, no residuals reweighting, no flattening, weak depth weighting with $D = 1$, with misfit: r.m.s. = $28 \text{ } \mu\text{Gal}$, max = $55 \text{ } \mu\text{Gal}$). Growth running screen with top and lateral views at the 3D model.

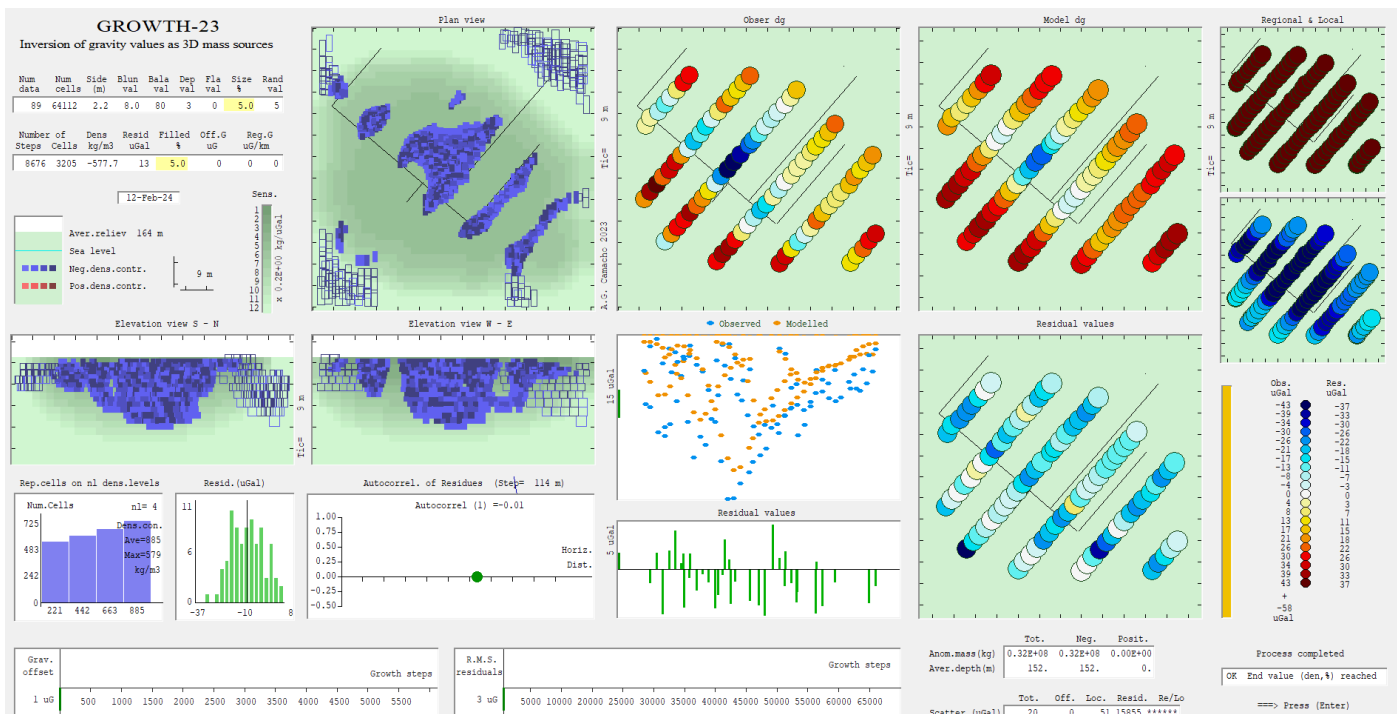


Figure C7

Over-compacted Growth solution with better data fit and lower average density contrast ($\lambda = 80$, % = 5.0, average $\Delta\rho = -578 \text{ kg/m}^3$, no residuals reweighting, no flattening, weak depth weighting with $D = 1$, with misfit: r.m.s. = $13 \text{ } \mu\text{Gal}$, max = $55 \text{ } \mu\text{Gal}$). Growth running screen with top and lateral views at the 3D model.

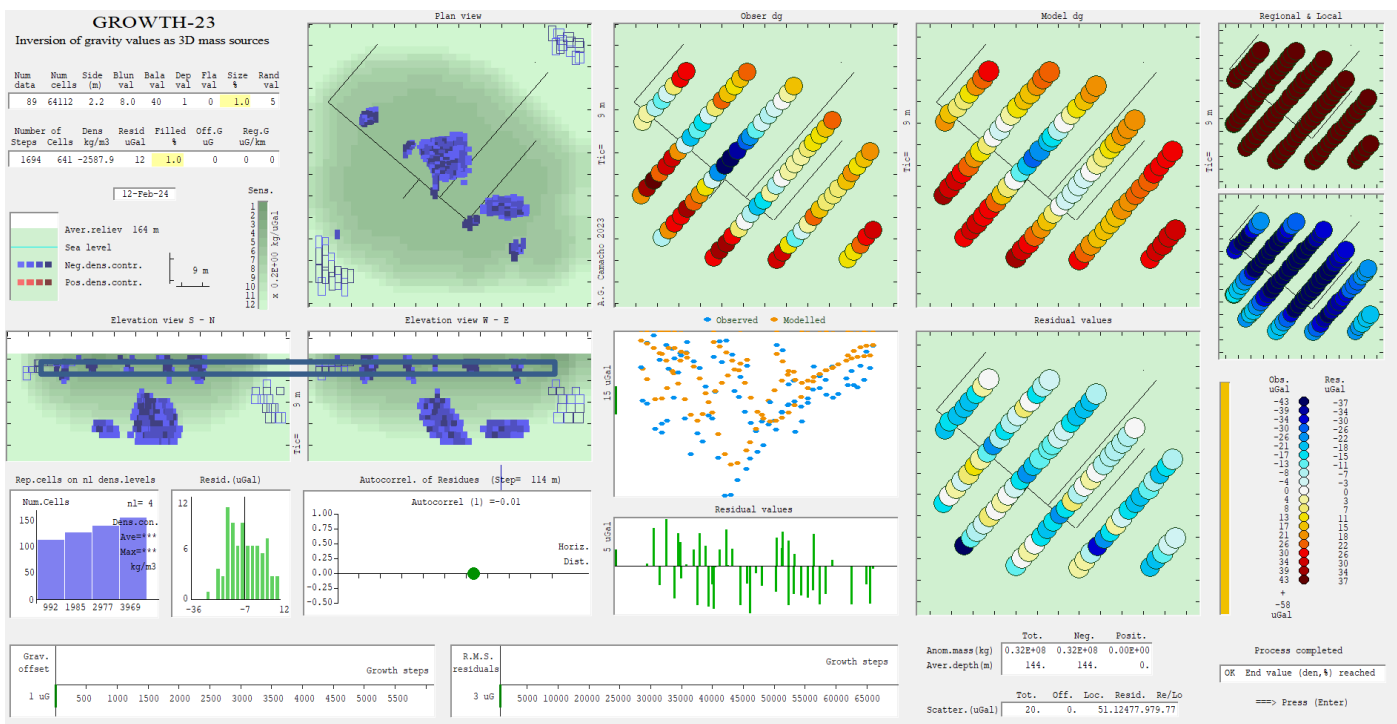


Figure C8

Growth solution with a fair data fit and average density contrast roughly related to void space ($\lambda = 40$, % = 1.0, average $\Delta\rho = -2588 \text{ kg/m}^3$, no residuals reweighting, no flattening, weak depth weighting with $D = 1$, with misfit: r.m.s. = $12 \text{ } \mu\text{Gal}$, max = $27 \text{ } \mu\text{Gal}$). Growth running screen with top and lateral views at the 3D model. This model appears as if the sources were aligned along two horizons.

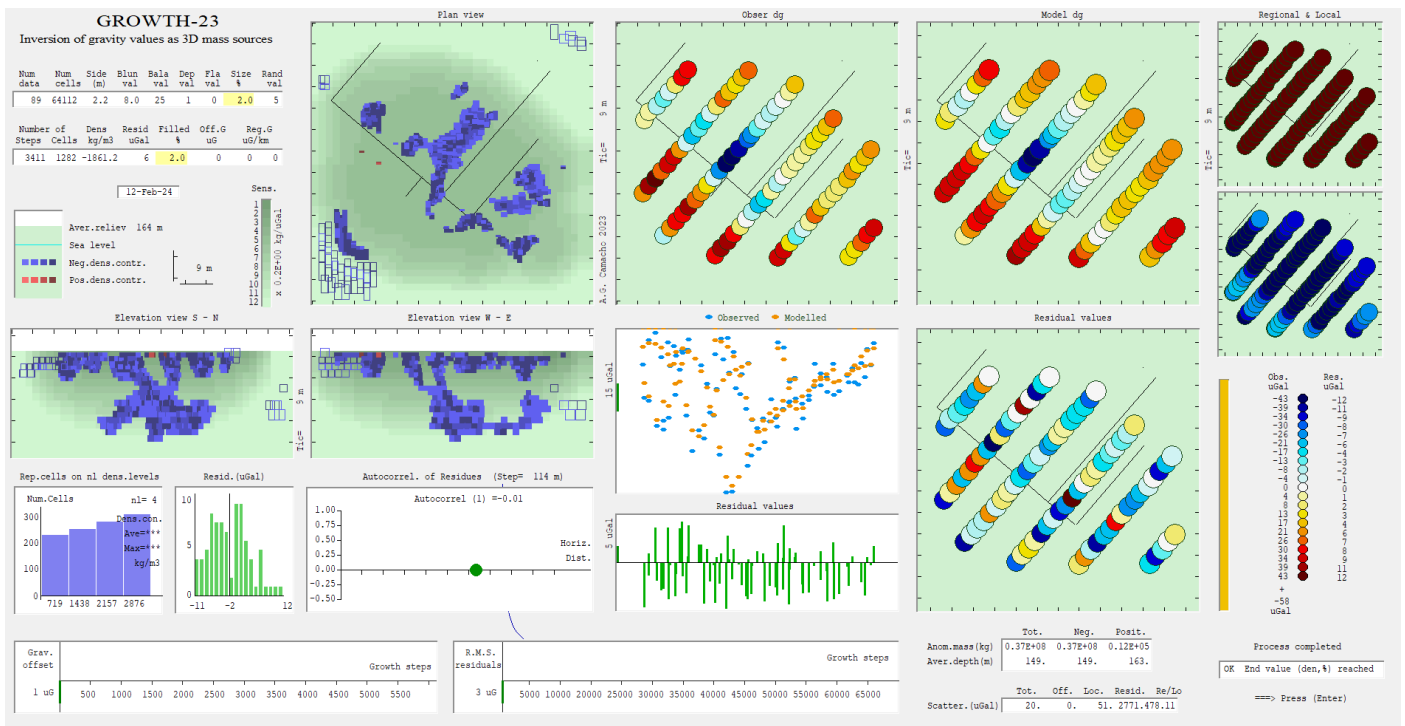


Figure C9

A tight-fitting (perhaps slightly overfitting) Growth solution
 $(\lambda = 25, \% = 2.0, \text{average } \Delta\rho = -1861 \text{ kg/m}^3, \text{no residuals reweighting, no flattening, weak depth weighting with } D = 1, \text{with misfit: r.m.s.} = 6 \text{ } \mu\text{Gal, max} = 12 \text{ } \mu\text{Gal}).$
 Growth running screen with top and lateral views at the 3D model.

All the Growth solutions for data on the truncated area, presented above, focusing on the deep source body, use weak depth weighting with $D = 1$. If no depth weighting is used, the deep source body is attached to the bottom boundary (at about 50 m below surface) of the model space respective to the truncated data area. This might indicate that the deep source body spans below the bottom boundary of the above models, i.e., below 50 m below surface, as is the case for Growth models for the whole data area that adopt no depth weighting.